Accepted Manuscript

Exploring the PROTAC degron candidates: OBHSA with different side chains as novel selective estrogen receptor degraders (SERDs)

Yuanyuan Li, Silong Zhang, Jing Zhang, Zhiye Hu, Yuan Xiao, Jian Huang, Chune Dong, Shengtang Huang, Hai-Bing Zhou

PII: S0223-5234(19)30286-7

DOI: https://doi.org/10.1016/j.ejmech.2019.03.058

Reference: EJMECH 11228

To appear in: *European Journal of Medicinal Chemistry*

Received Date: 15 January 2019

Revised Date: 23 March 2019

Accepted Date: 24 March 2019

Please cite this article as: Y. Li, S. Zhang, J. Zhang, Z. Hu, Y. Xiao, J. Huang, C. Dong, S. Huang, H.-B. Zhou, Exploring the PROTAC degron candidates: OBHSA with different side chains as novel selective estrogen receptor degraders (SERDs), *European Journal of Medicinal Chemistry* (2019), doi: https://doi.org/10.1016/j.ejmech.2019.03.058.

Exploring the PROTAC Degron Candidates: OBHSA with Different Side Chains as Novel Selective Estrogen Receptor Degraders (SERDs)

Yuanyuan Li, Silong Zhang, Jing Zhang, Zhiye Hu, Yuan Xiao, Jian Huang, Chune Dong,* Shengtang Huang,* and Hai-Bing Zhou*

A series of novel SERDs with excellent ER degradation efficacy have been discovered. These findings simplified the structure of currently available degrons and provide new possibility for discovering novel PROTACs.

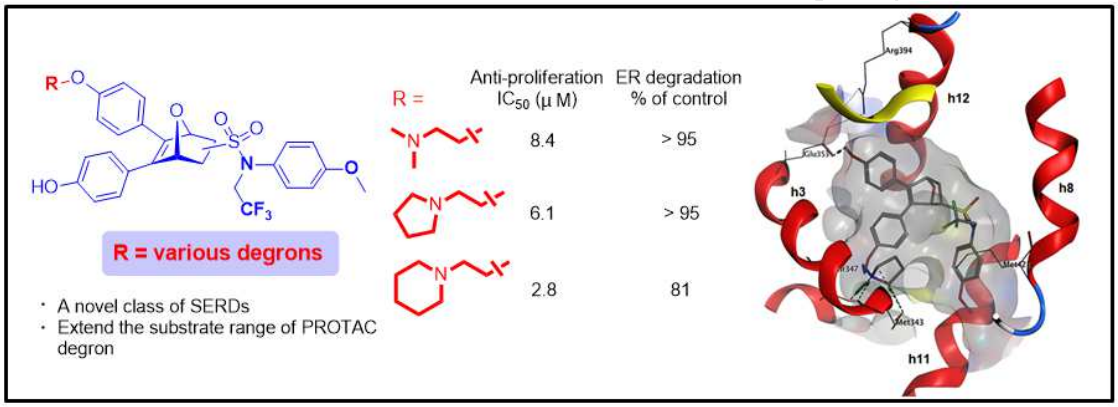

Exploring the PROTAC Degron Candidates: OBHSA with Different Side Chains as Novel Selective Estrogen Receptor Degraders (SERDs)

Yuanyuan Li,[1†] Silong Zhang,[1†] Jing Zhang,[1] Zhiye Hu,[1] Yuan Xiao,[1] Jian Huang,[3] Chune Dong,[1]* Shengtang Huang,[2*] and Hai-Bing Zhou[1]*

[1] State Key Laboratory of Virology, Hubei Province Engineering and Technology Research Center for Fluorinated Pharmaceuticals, Key Laboratory of Combinatorial Biosynthesis and Drug Discovery (Wuhan University), Ministry of Education, Wuhan University School of Pharmaceutical Sciences, Wuhan 430071, China; E-mails: zhouhb@whue.du.cn; cdong@whu.edu.cn

[2] The Lab of Cardiovascular, Cerebrovascular and Metabolic Disorder, Hubei University of Science and Technology, Xianning 437100, China; E-mail: huangst6511@hbust.edu.cn

[3] College of Life Sciences, Wuhan University, Wuhan 430072, China

[†] The authors contributed equally to this work.

Abstract

As the mutant estrogen receptor (ER) continues to be characterized, breast cancer is becoming increasingly difficult to cure when treated with hormone therapy. In this regard, a strategy to selectively and effectively degrade the ER might be an effective alternative to endocrine therapy for breast cancer. In a previous study, we identified a novel series of 7-oxabicyclo[2.2.1]heptene sulfonamide (**OBHSA**) compounds as full ER antagonists while lacking the prototypical ligand side chain that has been widely used to induce antagonism of ERα. Further crystal structure studies and phenotypic assays revealed that these compounds are selective estrogen receptor degraders (SERDs) with a new mechanism of action. However, from a drug discovery point of view, there still is room to improve the potency of these **OBHSA** compounds. In this study, we have developed new classes of SERDs that contain the **OBHSA** core structure and different side chains, e.g., basic side chains, long alkyl acid side chains, and glycerol ether side chains, to simply mimic the degrons of proteolysis targeting chimera (PROTAC) and then investigated the structure-activity relationships of these PROTAC-like hybrid compounds. These novel SERDs could effectively inhibit MCF-7 cell proliferation and demonstrated good ERα degradation efficacy. Among the SERDs, compounds **17d**, **17e** and **17g** containing a basic side chain with a *N*-trifluoroethyl substituent and a *para* methoxyl group at the phenyl group of the sulfonamide turned out to be the best candidates for ER degraders. A further docking study of these compounds with ERα elucidates their structure-activity relationships, which provides guidance to design new PROTAC degrons targeting ER for breast cancer therapy. Lastly, easy modification of these PROTAC-like SERDs enables further fine-tuning of their pharmacokinetic properties, including oral availability.

Keywords: SERDs, side chains, degrons, ER degradation

1. Introduction

It is well-known that the overexpression of estrogen receptor α (ERα) may lead to ER positive breast cancer, which accounts for 70% of breast cancer [1, 2]. Contraposing this target, clinical pharmacists generally use endocrine therapy, in which the drugs can be classified into two types: aromatase inhibitors (AIs) [3-5] and selective estrogen receptor modulators (SERMs) [2, 6-8]. However, the recurrence of breast cancer is difficult to treat, and the long-term use of SERMs, such as tamoxifen, is prone to lead to the development ovarian cancer and drug resistance [9-11], which is usually fatal. For patients who are on long-term medication, the limited number of effective drugs encourages the development of new compounds that reduce the likelihood of disease recurrence and drug resistance through various means.

Inducing protein degradation by small molecules has recently become a hot spot for drug discovery [12, 13]. To date, as the emerging and efficient treatments for breast cancer, there have been two approaches targeting ERα protein degradation: selective estrogen receptor downregulators (SERDs) and proteolysis targeting chimeras (PROTACs). SERDs are recognized as pure ER antagonists that can cause spatial structural instability and activate the ubiquitination pathway to degrade ERα protein [14-18]. In 2007, the FDA approved the first SERD fulvestrant for the treatment of advanced breast cancer [19]. Nevertheless, this SERD's low oral bioavailability limited its application [20]. Therefore, medicinal chemists hope to obtain SERDs with better oral bioavailability through structural modification and optimization. To date, a variety of SERDs have been identified [21-26], most of which have different side chains, e.g., long alkyl side chains, acrylic side chains, and basic side chains (**Figure 1**). Fulvestrant (**Figure 1**, compound **1**) is one typical drug that introduced a sulfinyl pentafluoro alkyl chain onto a E_2 skeleton; the hydrophobic chain was exposed to the surface of the protein when binding to ER and destabilized the active ligand binding domain (LBD) conformer, thereby leading to protein degradation. Therefore, Kurihara *et al.* reported that a derivative of tamoxifen with a long alkyl side chain (**Figure 1**, compound **2**) could effectively reduce ER protein levels in breast cancer cells and have an antagonistic effect [26]. Later,

these researchers expanded the range of currently available SERDs by attaching a decyl group to the amine moiety of raloxifene and revealed that the ER degradation efficacy of this compound is 1 μM [25]. GDC0810 (**Figure 1**, compound **3**), a second-generation SERD, contains an acrylic side chain, which directly interacted with the peptide backbone of ERα and induced a conformational change that exposed a hydrophobic surface on the receptor [27]. GDC0810 has undergone a clinical phase II trial and was effective in endocrine therapy to treat advanced metastatic ER^+ breast cancer; unfortunately, its clinical trial was recently discontinued. In 2018, Smith's group reported that derivatives of EM-652 that contained a basic side chain were highly potent and efficacious SERDs [18]. The best compound (**Figure 1**, compound **4**) of this series demonstrated robust activity with a 91% ERα degradation efficacy in a xenograft model of tamoxifen-resistant breast cancer. Moreover, the crystal structure study revealed that the side chains of these compounds may play an essential role in the degradation of ER, e.g., the acrylic acid side chain of **3**-type compounds formed a hydrogen bond with D351 in the ligand binding domain of ER, which blocked the proper positioning of the critical helix 12. Thus, hydrophobic patches were exposed in solution, the receptor was recognized by the ubiquitin-proteasome system and degradation proceeded [28]. For fulvestrant-type SERDs, when binding to ER, helix 12 appeared to be completely distorted, and the hydrophobic regions were exposed to solution for ubiquitination targeting. As a result, the side chain is a major driving factor of SERDs and plays a critical role in the degradation of ER.

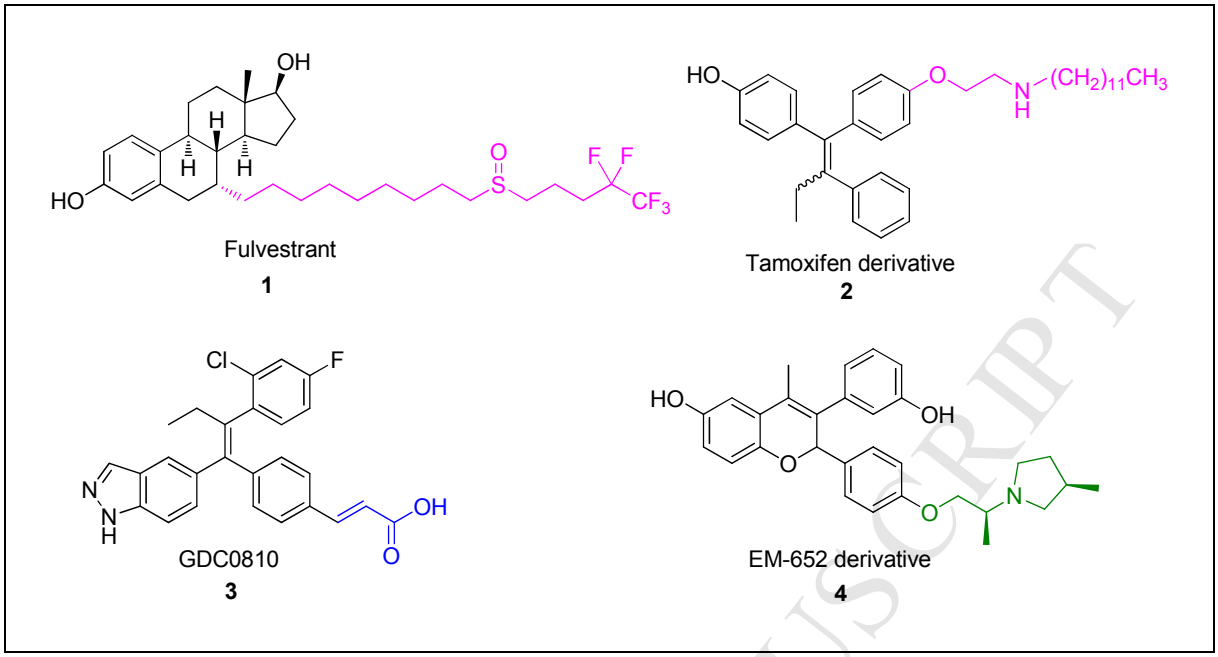

Figure 1. Four representative SERDs with typical side chains.

Another method for compounds capable of inducing protein degradation is proteolysis targeting chimeras (PROTACs). PROTAC is a bifunctional compound possesses a ligand for a targeted protein and a recognition motif for E3 ubiquitin ligase recruitment that ultimately promotes ubiquitination-dependent proteasomal degradation of the target protein. In 2010, an ER-targeting PROTAC that consisted of an estradiol and a hypoxia-inducing factor 1α (HIF-1α)-derived synthetic pentapeptide was reported [29], which showed good ER binding affinity (10% binding affinity relative to E2) and effective ER degradation efficacy (60% ER degradation). Kurihara *et al.* disclosed a complex comprised of 4-hydroxytamoxifen and bestatin (an inhibitor of the cIAP1) via an alkyl linker [30]. This complex induced cIAP1-mediated ubiquitination of ERα with proteasomal degradation at 10 μM. Recently, Li *et al.* reported a novel ERα-targeting PROTAC that was composed of an *N*-terminal aspartic acid cross-linked stabilized peptide ERα modulator (TD-PERM) and the Von Hippel-Lindau (VHL) E3 ubiquitin ligase through a pentapeptide [31]. The TD-PROTAC approach utilized a peptide stabilization strategy, which could provide peptide conjugates with satisfactory stability and cellular uptake. However, the effective dose for degradation is 20 μM, which still needs improvement. Generally, PROTACs are under rapid development as a novel and promising technology for drug discovery [32-34]. Nonetheless, there is a very narrow

selection of the structural species for PROTACs targeting ER degradation, and their low potency limits their clinical trials.

Despite the different mechanisms for degrading ER by SERDs and PROTACs, these compounds have a molecular skeleton that induces ER degradation and could be called a degron. A degron is reported to be a part of the ligand-induced degradation (LID) domain in known works, and it functions as a cryptic degradation sequence [35, 36]. Recently, Sharma's group reported a series of new SERDs that extended the currently available library of PROTAC-type scaffolds, which may be useful for the degradation of a variety of other therapeutically important proteins [16]. The researchers defined the special motif that can induce ER degradation as a degron in both SERDs and PROTAC molecules. As the skeletons of the PROTAC degrons are limited and always complicated, there is an urge to explore novel degrons with diverse and simple structures that allow the ER degrader to display drug-like properties and more potent efficacy. In 2012, our group reported oxabicycloheptene sulfonamide (**OBHSA**, **Figure 2**) compounds as full ER antagonists [37], and further study on the crystal structures of complexes of these ligands with ERα revealed a new mechanism of action of these SERD compounds [38]. The large R^2 groups (*N*-trifluoroethyl group and *N*-ethyl group) clashed strongly with Leu525, inducing a 2.5 Å shift in h11 and leading to the complete disorder of the C terminus of h11. Thus, h12 Leu544 moved out of the hydrophobic groove. In addition, the 4-methoxyphenyl substitution flipped the ethyl and aryl groups around the sulfonamide linker and interacted with the loop between h7 and h8 by attacking the backbone carbonyl of Glu419. Therefore, under the influence of the disordered h11 and h12 exposed in the hydrophilic environment, the ER protein would become a target for ubiquitination. Considering the important role played by the sulfonamide moiety in this new mechanism, we turn our attention to the phenol group on the other side, hoping to develop new degrons on the phenolic group that would contribute to the degradation activity. As part of our long-term interests in the development of ER ligands [39-41], we utilized the **OBHSA** as a core structure and explored alternatives of degrons to, for example, the basic side chains, long alkyl acid side chains, and glycerol ether side chains, and then, we investigated their

inhibition efficacy of MCF-7 cell proliferation and ERα degradation activity. In the process, we uncovered some remarkable structure-activity relationships (SARs) in which compounds **17d**, **17e** and **17g** containing basic side chains with *N*-trifluoroethyl and *para* methoxy substituents displayed outstanding ERα degradation efficacy and anti-proliferation activity. Further docking analysis illustrates that the basic side chain could distort helix 3 by forming a hydrogen bond with Thr347 and a hydrophobic repulsion with the backbone of Met343. The *N*-trifluoroethyl group and the *para* methoxyl group may also be beneficial to the ERα degradation efficacy by influencing the loop of helix 7 and helix 8. The results indicate that the basic side chain proved to be the best degron and provides new possibilities in the development of more effective PROTACs.

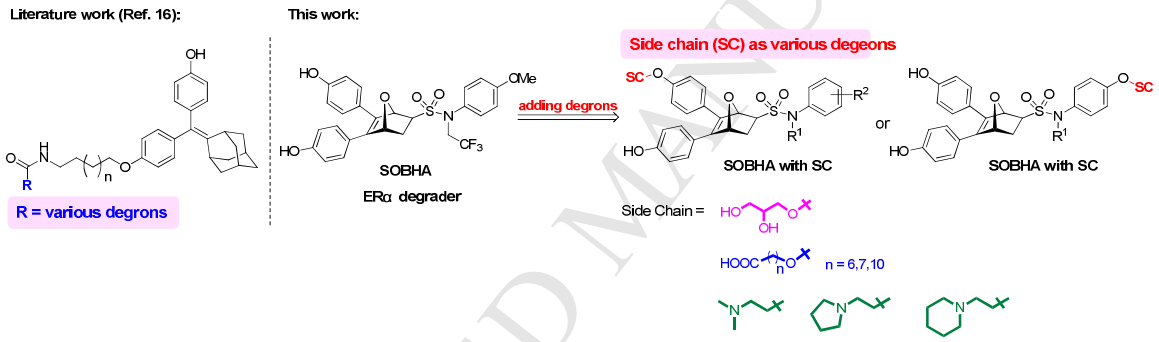

Figure 2. Design of **OBHSA** derivatives with different degrons as SERDs.

2. Results and discussion

2.1 Chemistry

The synthesis of the final **OBHSA** derivatives **17a-t** involved a Diels-Alder reaction between a series of furan analogues and ethylene sulfonamide derivatives (**Scheme 4**), and the furan intermediate **7** was synthesized according to our previous work [42]. To introduce different degrons onto the **OBHSA** pharmacophore core, we synthesized the key intermediates **8a-j**, and the synthetic route is shown in **Scheme 1**. The furan analogues **8a-g** were obtained by Williamson etherification reactions with different halogenated compounds, and the hydrolysis of the compounds **8e-g** created the furan analogues **8h-j**.

Scheme 1. Synthesis of furan derivatives **8a-j**[a].

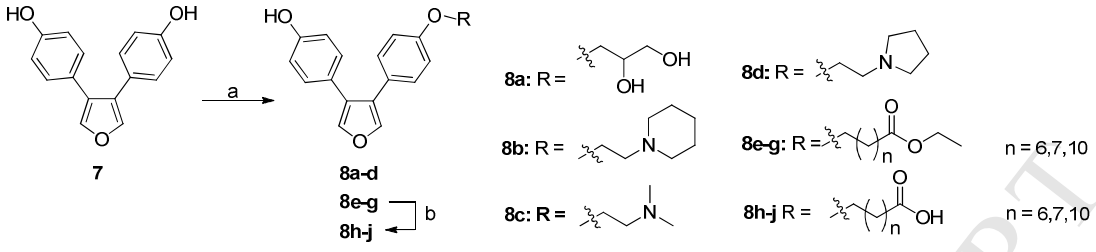

[a] Reagents and conditions: (a) 2-chloro-*N*,*N*-dimethylethanamine hydrochloride, 1-(2-chloroethyl)pyrrolidine hydrochloride, 1-(2-chloroethyl)piperidine hydrochloride, 3-chloropropane-1,2-diol, ethyl 11-bromoundecanoate, ethyl 8-bromooctanoate, or ethyl 7-bromoheptanoate, KOH, CH_3CN, 60 °C, 6 h; (b) LiOH, MeOH, rt, 4 h**.**

In a previous study, it was indicated that the trifluoroethyl group and *para* methoxyl group played an important role for the binding and degradation of the **OBHSA** compounds [38], and as such, our synthesis mainly focused on the *N*-trifluoroethyl group and *para* substitution of the phenyl of sulfonamide. Ethylene sulfonamide derivatives **14a-f** were synthesized as shown in **Scheme 2**. The substituted anilines **9a-d** yielded analogs **10a-e** through an amidation reaction with acetic anhydride or trifluoroacetic anhydride in the presence of DMAP. The compound **10a** was treated with methyl iodide to yield *N*-methyl phenylacetamide **11**. Then, the intermediate **12** was obtained by the deacylation of **11** after refluxing for 24 h in 10% HCl and glycol. Finally, the key intermediate **14a** was gained through the reaction of **12** with 2-chloroethanesulfonyl chloride in the presence of TEA. For the synthesis of ethylene sulfonamides **14b-f**, the route was slightly different. Compounds **10a-e** were reduced by $BH_3{\cdot}SMe_2$ in THF at 60 °C to give **13a-e**. Then, following the reaction with 2-chloroethanesulfonyl chloride, dienophiles **14b-f** were obtained.

Scheme 2. Synthesis of dienophiles **14a-g**[a].

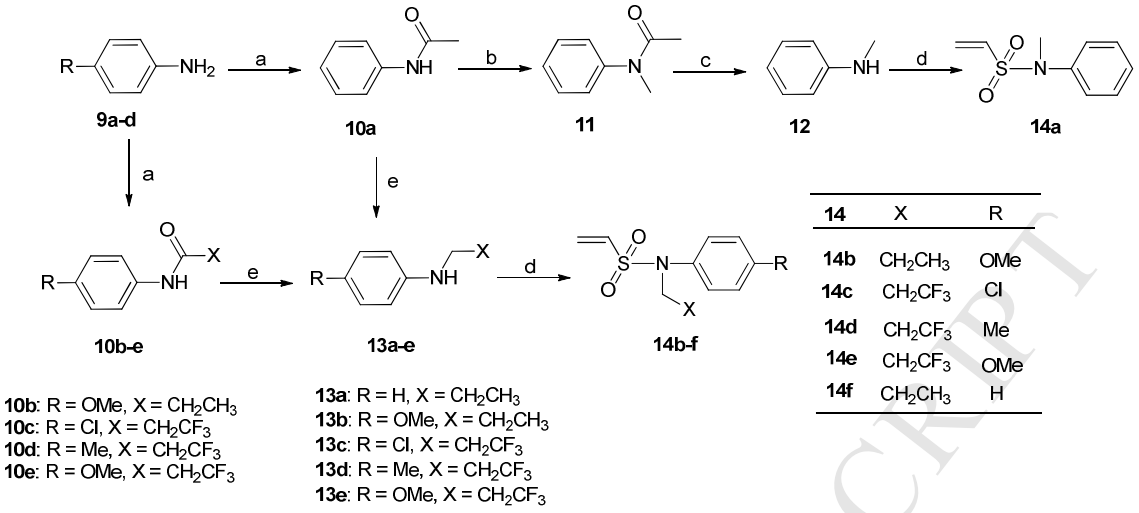

14	X	R
14b	CH_2CH_3	OMe
14c	CH_2CF_3	Cl
14d	CH_2CF_3	Me
14e	CH_2CF_3	OMe
14f	CH_2CH_3	H

[a] Reagents and conditions: (a) acetic anhydride or trifluoroacetic anhydride, rt, 3 h; (b) MeI, NaH, THF, 0 °C, 4 h; (c) 10% HCl, $HO(CH_2)_2OH$, reflux, 3 h; (d) 2-chloroethanesulfonyl chloride, 20% NaOH, DCM, 0 °C, 24 h; (e) $BH_3 \cdot SMe_2$, THF, 60 °C, 24 h.

The ethylene sulfonamides with different side chains were obtained from the intermediate **14b**. After the demethylation of compound **14b** with BBr_3, product **15** interacted with 3-chloropropane-1,2-diol, alkyl ester bromides, or 1-(2-chloroethyl)piperidine hydrochloride through Williamson etherification and yielded the dienophiles **16a-e**. Compounds **16f-h** with long alkyl acid chains were obtained by the hydrolysis of esters **16c-e** (**Scheme 3**).

Scheme 3. Synthesis of ethylene sulfonamides with different side chains[a].

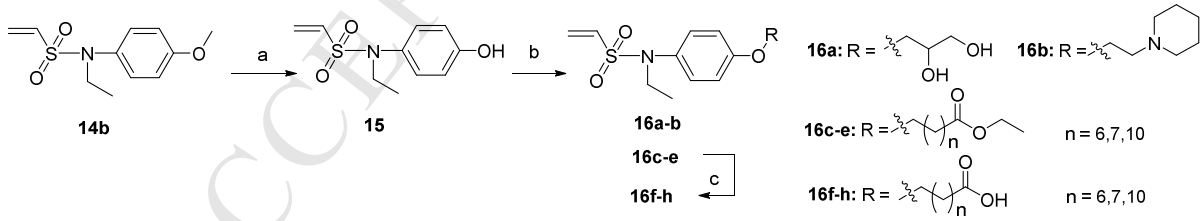

[a] Reagents and conditions: (a) BBr_3, CH_2Cl_2, -20 °C, 12 h; (b) 3-chloropropane-1,2-diol, ethyl 11-bromoundecanoate, ethyl 8-bromooctanoate, ethyl 7-bromoheptanoate, or 1-(2-chloroethyl)piperidine hydrochloride, KOH, CH_3CN, 60 °C, 6 h; (c) LiOH, MeOH, rt, 4 h.

The final step was the Diels-Alder reaction between different furan analogues and dienophiles (**Scheme 4**). All of the compounds gave moderate to good yields. It is worth noting that a high

stereoselectivity was obtained in the cycloaddition reaction, as we have observed previously [43, 44]. In this study, the thermodynamically favorable *exo* products of **17a-t** were more easily generated through this Diels−Alder reaction, which was presumed to be due to the high rate and easy reversibility, while the *endo* isomers were hardly found. In addition, among compounds **17a-q**, compounds **17b**, **17d**, **17f**, **17g** and **17j** are mixtures of two regioisomers, while the others are obtained as single isomers. The ratios of regioisomers were determined from the corresponding ^{1}H NMR, and the structures and stereoisomeric assignments of the single isomers were analyzed by NOESY-NMR (see the Experimental Section and Supporting Information for details).

Scheme 4. Synthesis of **OBHSA** derivatives **17a-t**.

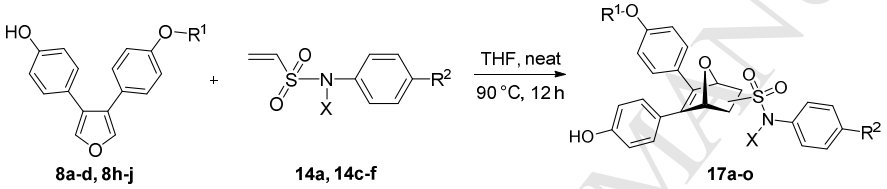

8a-d, 8h-j **14a, 14c-f** **17a-o**

17a-i	R^1	X	R^2	Yields[a] (ratio of regioisomers)
17a	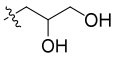	CH_2CH_3	H	61%
17b		CH_2CF_3	OCH_3	74% (4:1)
17c		CH_2CF_3	Cl	56%
17d	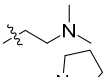	CH_2CF_3	OCH_3	75% (5:1)
17e	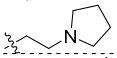	CH_2CF_3	OCH_3	72%
17f	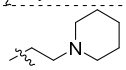	CH_2CF_3	CH_3	72% (4:1)
17g		CH_2CF_3	OCH_3	70% (3:1)
17h		CH_3	H	81%
17i		CH_2CH_3	H	75%

17j-o	R^1	X	R^2	n	Yields[a] (ratio of regioisomers)
17j	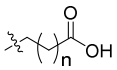	CH_2CH_3	H	6	60% (3:1)
17k		CH_2CH_3	H	7	63%
17l		CH_2CH_3	H	10	69%
17m		CH_2CF_3	4-OCH_3	6	68%
17n		CH_2CF_3	4-OCH_3	7	70%
17o		CH_2CF_3	4-OCH_3	10	59%

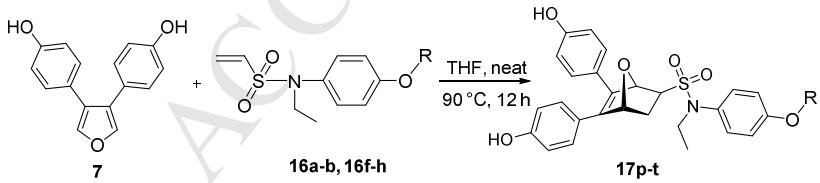

7 **16a-b, 16f-h** **17p-t**

17p-t	R	n	Yields (%)
17p	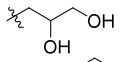		76%
17q	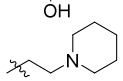		78%
17r	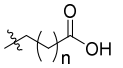	6	73%
17s		7	70%
17t		10	72%

[a]Unless noted, all of the products are a single isomer.

2.2 Biological testing

To explore the biological activities of these compounds, we utilized three assays to evaluate the biological properties. Their relative binding affinities for ERα were tested by the

competitive fluorometric receptor-binding assay. Their anti-proliferative activities on the MCF-7 cell line were evaluated using the MTT (3-(4,5-dimethylthiazol-2-yl)-2,5-diphenyltetrazolium bromide) assay, and their ERα degradation was assessed by Western blot assays.

2.2.1 Relative binding affinity

All of the binding affinities of the synthesized compounds for both ERα and ERβ were determined by a competitive fluorometric receptor-binding assay using methods that have been previously described [41], and the results are presented in **Table 1** (absolute affinities for estradiol: K_d 3.49 nM on ERα and 4.12 nM on ERβ). The affinities are presented as the relative binding affinity (RBA) values, with the binding affinity of estradiol being set at 100%.

In general, most of the synthesized compounds were ERα selective and exhibited modest affinities toward ERα, as well as low affinities toward ERβ. From entries 1-3 and 16, we can find that the compounds with a glycerol ether side chain demonstrated modest binding activities for ERα (RBA values were 0.26-1.94) and low affinities for ERβ (RBA values were less than 0.6). Furthermore, compound **17c**, which had no affinity toward ERβ, displayed the highest ERα selectivity among the whole series (α/β ratio was greater than 162), while analog **17p** showed slight ERβ selectivity (α/β ratio was 0.87).

Compounds with basic side chains (compounds **17d-i**) exhibited relatively high binding affinities for ERα and poor affinities for ERβ (**Table 1**, entries 4-9, RBA values were 0.95-3.25 for ERα and 0.12-0.81 for ERβ), except for compound **17e** (RBA values were 2.12 for ERα and 1.81 for ERβ). The best compound **17f** showed binding affinities of 3.25 for ERα and 0.12 for ERβ, respectively, thus providing a high ERα selectivity of 27. Nevertheless, the analogue **17h** with a *N*-methyl group demonstrated a relatively lower binding affinity for ERα (**Table 1**, entry 8, RBA value was 0.95) compared to other analogs with basic side chains. Comparing the size of the *N*-substituents (analogues **17h**, **17i** and **17d-g**), we also found that the higher binding affinity comes as a consequence of increasing the size of the *N*-substitute

from CH_3 to CH_2CF_3, which may be caused by that the trifluoroethyl substituent can stretch into the loop of helix 7 and helix 8 in the pocket of ERα and lead to steric strain (see discussion in the molecular docking section for details).

Compounds **17j-o** and **17r-t** (**Table 1**, entries 10-15 and entries 18-20) that contain long alkyl acidic chains displayed poor to modest binding activities toward ERα (RBA values were 0.06-3.21) and poor affinities toward ERβ (RBA values were less than 0.5). Comparison of the ERα binding affinities of **17l**, **17n**, **17o** and **17t** (RBA values were 0.06-0.93) to those of **17j**, **17k**, **17m**, **17r** and **17s** (RBA values were 1.20-3.21) indicates that the longer the chain length, the lower the binding affinity.

Table 1. Relative binding affinities (RBAs) of the compounds **17a-t** to ERα and ERβ.

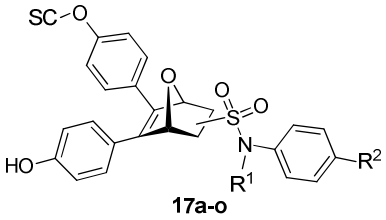

17a-o

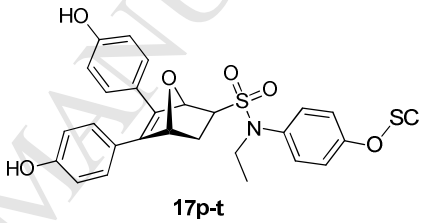

17p-t

Entry	Cmpd	Side chain	R^1	R^2	n	RBA[a] (%) ERα	RBA[a] (%) ERβ	α/β ratio
1	**17a**	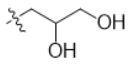	CH_2CH_3	H		0.26 ± 0.03	0.28 ± 0.02	0.94
2	**17b**		CH_2CF_3	OCH_3		1.94 ± 0.31	0.26 ± 0.05	7.52
3	**17c**		CH_2CF_3	Cl		1.62 ± 0.10	< 0.01	> 162
4	**17d**	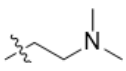	CH_2CF_3	OCH_3		1.71 ± 0.41	0.40 ± 0.07	4.28
5	**17e**	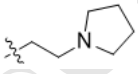	CH_2CF_3	OCH_3		2.12 ± 0.68	1.81 ± 0.08	1.17
6	**17f**	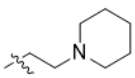	CH_2CF_3	CH_3		3.25 ± 0.75	0.12 ± 0.03	27.08
7	**17g**		CH_2CF_3	OCH_3		2.94 ± 0.22	0.37 ± 0.001	7.95
8	**17h**		CH_3	H		0.95 ± 0.17	0.79 ± 0.11	1.21
9	**17i**		CH_2CH_3	H		2.51 ± 0.17	0.81 ± 0.01	3.10
10	**17j**	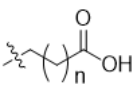	CH_2CH_3	H	6	2.48 ± 0.05	0.46 ± 0.02	5.39
11	**17k**		CH_2CH_3	H	7	1.20 ± 0.63	0.40 ± 0.04	3.00
12	**17l**		CH_2CH_3	H	10	0.93 ± 0.08	0.13 ± 0.002	7.10
13	**17m**		CH_2CF_3	OCH_3	6	1.82 ± 0.04	0.13 ± 0.07	13.68
14	**17n**		CH_2CF_3	OCH_3	7	0.07 ± 0.001	< 0.01	> 7
15	**17o**		CH_2CF_3	OCH_3	10	0.06 ± 0. 002	0.70 ± 0.20	0.09

16	**17p**	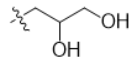				0.46 ± 0.07	0.53 ± 0.20	0.87
17	**17q**	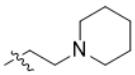				0.58 ± 0.09	0.25 ± 0.07	2.28
18	**17r**	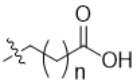			6	1.22 ± 0.03	0.41 ± 0.03	2.98
19	**17s**				7	3.21 ± 0.52	0.42 ± 0.03	7.64
20	**17t**				10	0.57 ± 0.01	< 0.01	> 57

[a]Relative binding affinity (RBA) values are determined by competitive fluorometric binding assays and are expressed as $IC_{50}^{estradiol}/IC_{50}^{compound} \times 100 \pm$ the range (RBA, estradiol = 100%).

2.2.2 Cell viability assay.

To evaluate their inhibition of breast cancer cell proliferation, all of the compounds were screened against the MCF-7 breast cancer cell line (**Table 2**). As a global observation, all compounds exhibited moderate to good anti-proliferation activity except for compound **17r** (**Table 2**, entry 18, IC_{50} value was greater than 50 μM), and some of them performed better than 4-hydroxytamoxifen.

Compounds with a glycerol ether side chain (**Table 2**, entries 1-3 and 16, compounds **17a-c** and **17p**) displayed modest potencies, and the anti-proliferative activities of **17b** and **17c** (IC_{50} values were 17.0 and 16.8 μM, respectively) were superior to those of **17a** and **17p** (IC_{50} values were 33.6 and 32.3 μM, respectively), which may be explained by the favorable interaction of the trifluoroethyl group with Met421 in the ER binding pocket, and this will be discussed in the molecular docking section.

Among the **OBHSA** derivatives that contain different basic side chains (**Table 2**, entries 4-9 and 17, compounds **17d-i** and **17q**), compounds **17f** and **17g** demonstrated the best anti-proliferative activities with IC_{50} values of 3.0 and 2.8 μM, respectively, which were also the most potent analogs among all compounds. In terms of compounds **17b**, **17d**, **17e**, **17g**, **17m**, **17n** and **17o** (**Table 2**, entries 2, 4-5, 7 and 13-15), one can see that the compounds **17d**, **17e**, and **17g** with basic side chains (**Table 2**, entries 4-5, and 7) showed better anti-proliferative activities (IC_{50} values were 8.4, 6.1, and 2.8 μM, respectively) than compounds with long alkyl acidic side chains (**17m**, **17n**, and **17o**, IC_{50} values were 15.9, 40.1, and 14.3 μM, respectively) and the glycerol ether side chain (**17b**, IC_{50} value was 17.0 μM). When the trifluoroethyl group was introduced on the *N*-position of the sulfonamide,

comparing compounds **17f-i** (**Table 2**, entries 6-9), the better efficacies of **17f** and **17g** than those of **17h** and **17i** were revealed in an anti-proliferation assay (**Table 2**, entries 6-7 vs 8-9). In general, among all of the compounds investigated except **17n**, the compounds with a trifluoroethyl group demonstrated good to the best activity against MCF-7 cells.

Among the analogues that contain long alkyl acidic side chains (**Table 2**, entries 10-15 and 18-20), the best compounds were **17l**, **17o** and **17t** with IC_{50} values of 10.3, 14.3 and 18.4 μM, respectively, which may uncover that the undecanoic acid chain (n = 10) was better than the octanoic acid chain (n = 7) and the heptanoic acid chain (n = 6).

Table 2. The anti-proliferative activity against MCF-7 cells.

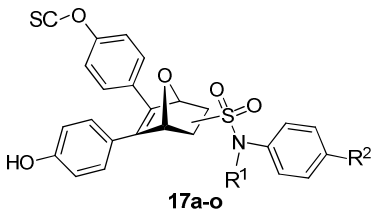

17a-o

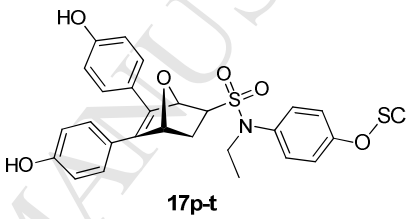

17p-t

Entry	Comp	Side chain	R^1	R^2	n	IC_{50} (μM)[a]
1	**17a**	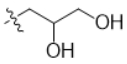	CH_2CH_3	H		33.6 ± 1.83
2	**17b**		CH_2CF_3	OCH_3		17 ± 1.39
3	**17c**		CH_2CF_3	Cl		16.8 ± 2.27
4	**17d**	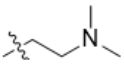	CH_2CF_3	OCH_3		8.4 ± 0.55
5	**17e**	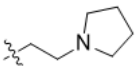	CH_2CF_3	OCH_3		6.1 ± 0.86
6	**17f**	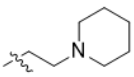	CH_2CF_3	CH_3		3.0 ± 0.03
7	**17g**		CH_2CF_3	OCH_3		2.8 ± 0.25
8	**17h**		CH_3	H		15.2 ± 0.16
9	**17i**		CH_2CH_3	H		12.9 ± 0.74
10	**17j**	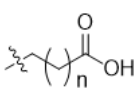	CH_2CH_3	H	6	34.6 ± 0.41
11	**17k**		CH_2CH_3	H	7	27.4 ± 0.54
12	**17l**		CH_2CH_3	H	10	10.3 ± 0.20
13	**17m**		CH_2CF_3	OCH_3	6	15.9 ± 0.41
14	**17n**		CH_2CF_3	OCH_3	7	40.3 ± 4.81
15	**17o**		CH_2CF_3	OCH_3	10	14.3 ± 0.76
16	**17p**	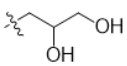				32.3 ± 3.16

17	**17q**	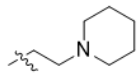				5.4 ± 0.29
18	**17r**	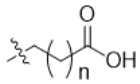			6	>50[b]
19	**17s**				7	24.9 ± 0.29
20	**17t**				10	18.4 ± 0.44
21	4-OHT					10.1 ± 0.34

[a] IC_{50} values are an average of at least three independent experiments ± standard deviation (mean ± SD). [b] IC_{50} not determinable up to the highest concentrations tested.

2.2.3 ERα degradation assay

The ERα degradation assay of the synthesized compounds has been further investigated. Considering the anti-proliferation ability of this series of compounds, we used 10 μM of each compound to test the ERα level. The Western blot results of synthesized **OBHSA** analogs with different degrons have been presented in **Figure 3A-C**. All of the bands were quantitatively analyzed by Quantity One, and the results are given in **Figure 3D**. Comparing compounds **17a-c** and **17p** that contained the glycerol ether side chain (**Figure 3A**), compounds **17b-c** with a *N*-trifluoroethyl group demonstrated modest degradation efficacies (the ERα levels were 41% and 38%, respectively). For the analogs that contained basic side chains (**Figure 3B**), compounds **17d**, **17e**, and **17g** could efficiently degrade ERα with 99%, 99% and 81% degradation efficacies, respectively. However, when treated with compounds **17f**, **17h**, **17i** and **17q**, the ERα levels were 102%, 98%, 95% and 89%, which indicated that these analogs were essentially inactive against ERα degradation. A further docking study showed that the basic side chain could influence helix 3 with noncovalent repulsion to Thr347 and Met343. The *N*-trifluoroethyl group and the *para* methoxyl group may also support ERα degradation by clashing with Met421 on the loop of helix 7 and helix 8. These combined influences might contribute to the good degradation activities of compounds **17d**, **17e** and **17g**. From the results when treated with compounds containing long alkyl acidic side chains (**Figure 3C**), the compounds **17m**, **17n** and **17t** (side chain lengths were 6, 7 and 10, respectively) showed modest activities (ER levels were 32%, 42% and 29%, respectively), which indicated that the length of the long alkyl acidic side chain had no influence on the ERα degradation efficacy.

Lastly, in order to verify that the degradation activities of these novel PROTACs are likely mediated mainly by the side chains, we chose the best compound **17e** of the series for comparison with the parent compound **OBHSA-1** and conducted an ERα degradation assay with different concentrations hoping to obtain an approximate ERα degradation potency of this compound. We chose concentrations of 0.1 μM, 0.5 μM, 1 μM, 5 μM, and 10 μM and compared them with the essential control **OBHSA-1** (**Figure 3E**). The results revealed that compound **17e** demonstrated better results than **OBHSA-1**. Compound **17e** can completely degrade ERα at 1 μM, and it showed good degradation activity at 0.5 μM. Meanwhile, OBHSA-1 showed complete degradation at 5 μM, which indicated that the basic side chain of compound **17e** played an important role in increasing the degradation potency on ERα.

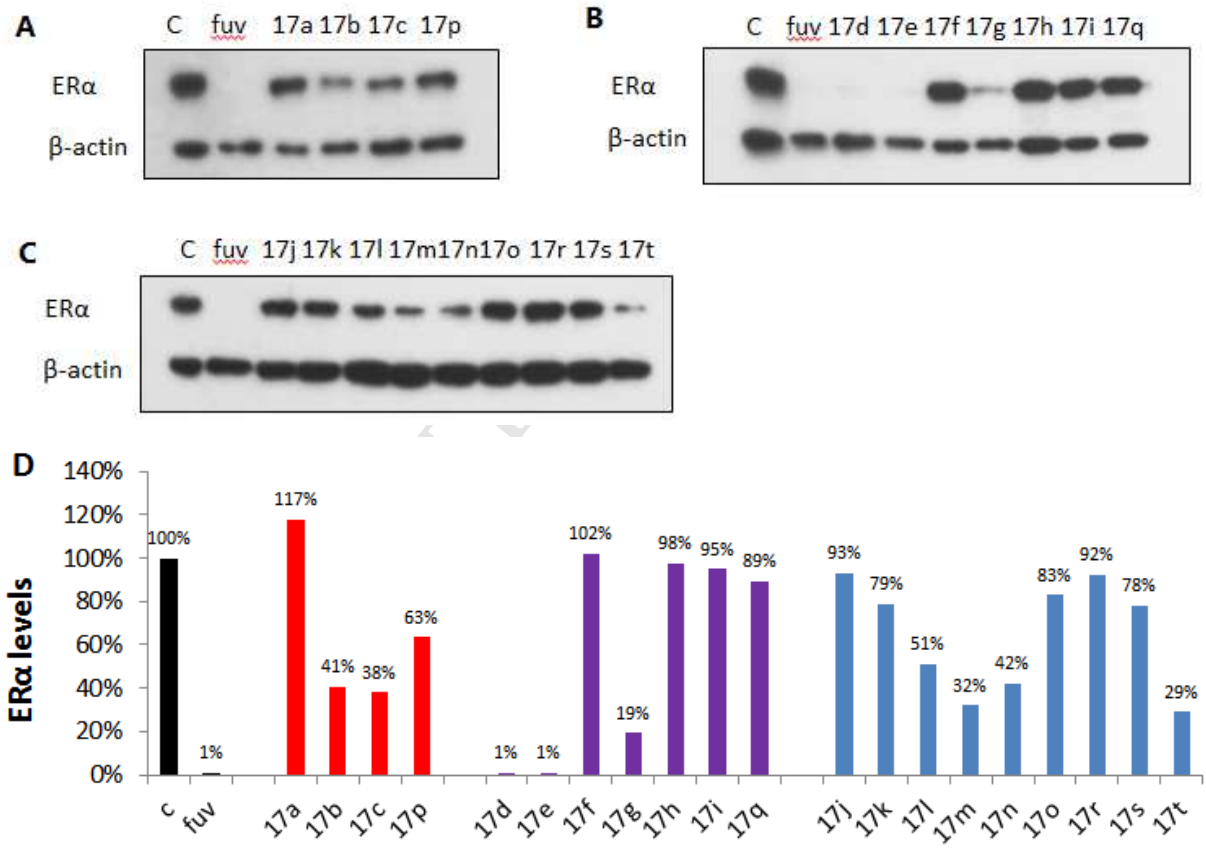

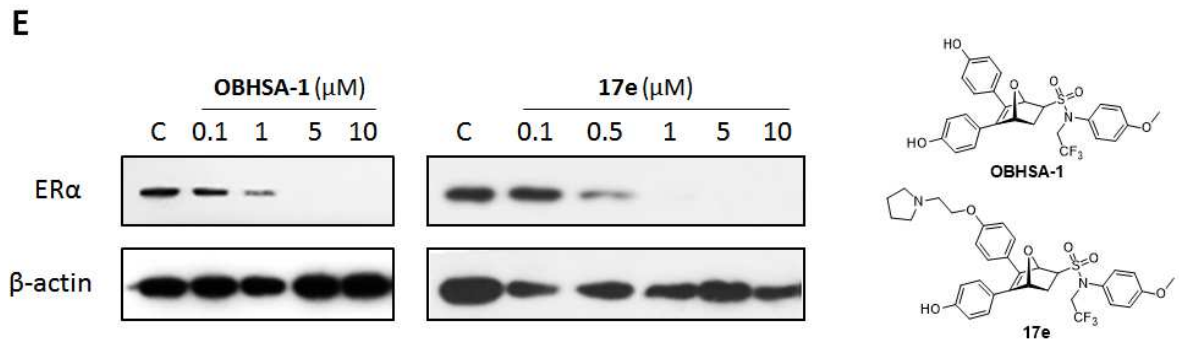

Figure 3. Western blot assay of ERα in MCF-7 cells treated by compounds with (**A)** a glycerol ether side chain, (**B**) basic side chains and (**C**) long alkyl acidic side chains. (**D**) The graph exhibits ERα values for **17a-t**. Cells were incubated with DMSO or the compound (10 μM) for 20 h. The whole proteins were extracted, and the ERα protein levels were analyzed by Western blotting. (**E**) Western blot assay of ERα treated with **OBHSA-1** and **17e** in different doses from 0.1 μM to 10 μM.

*2.4 Structure-activity relationships of the **OBHSA** derivatives*

To more intuitively observe the effects of different degrons on the biological activities of the compounds, we made a scatter plot based on the anti-proliferative activity and ERα degradation efficacy (**Figure 4A**). For the ERα degradation assay, as a global observation, compounds that contain basic side chains (**17d**, **17e**, and **17g**, red spots) demonstrated excellent ERα degradation efficacies, which indicated that the basic side chains were the best degrons for ER degradation. Most of the green spots and the blue spots were distributed in the middle or up the figure, from which we can conclude that the long alkyl acidic side chain and the glycerol ether side chain possess a weak influence on ER degradation. However, compounds **17f**, **17q**, **17i** and **17h**, which also contain basic chains, didn't demonstrate potency to degrade ER. Our data suggests that the basic side chain degron might be a major driving factor of ERα degradation activity; however, it appears to require a combination of influences of other substituents in these types of compounds through a distinct mechanism of action, which could be illustrated in the further docking analysis. Additionally, the length of

the alkyl acidic side chain did not affect the ERα degradation efficacy, as indicated by comparing compounds **17j-o** (green spots).

In terms of the anti-proliferative activity, a similar trend as the efficacy of ERα degradation was observed. All of the compounds that contain basic side chains (red spots) demonstrated less than 20 μM IC_{50} values against MCF-7 cell lines, which indicated that the basic chain could help to inhibit the growth of breast cancer cells. Meanwhile, compounds with the long alkyl acidic side chain (green spots) and the glycerol ether side chain (blue spots) showed modest activities, and the majority of them exhibited IC_{50} values greater than 20 μM. Moreover, comparison of analogs **17l**, **17o** and **17t** (green spots, chain length = 10) with **17j**, **17k**, **17n**, **17r** and **17s** (green spots, chain length = 6 and 7) may uncover that the longer the chain length, the more potent the anti-proliferative activity. Taking all of the results and data into account, we summarized the structure-activity relationships of the **OBHSA** compounds in **Figure 4B**.

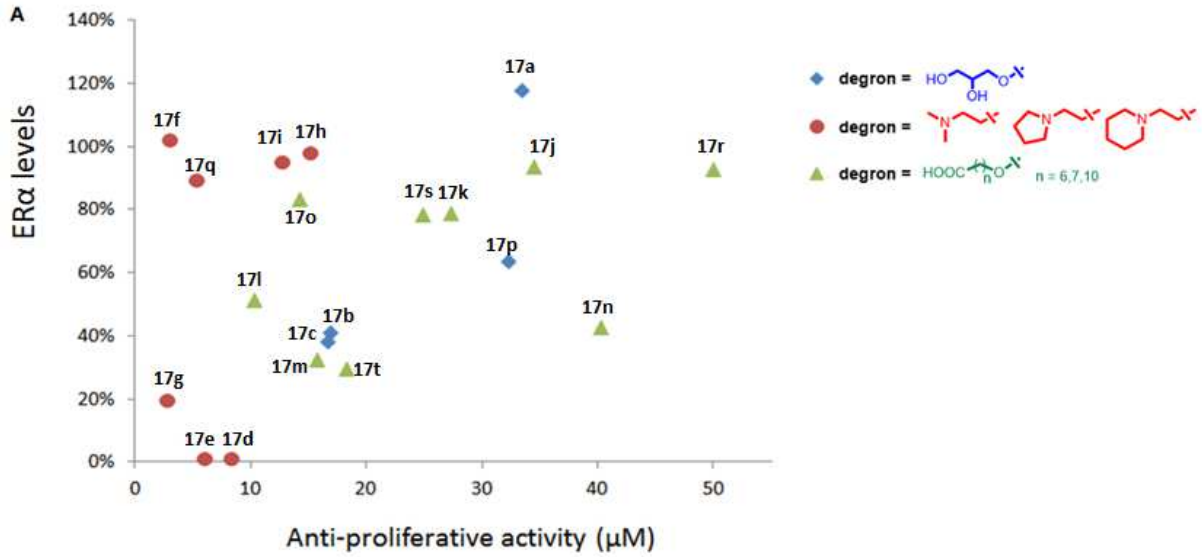

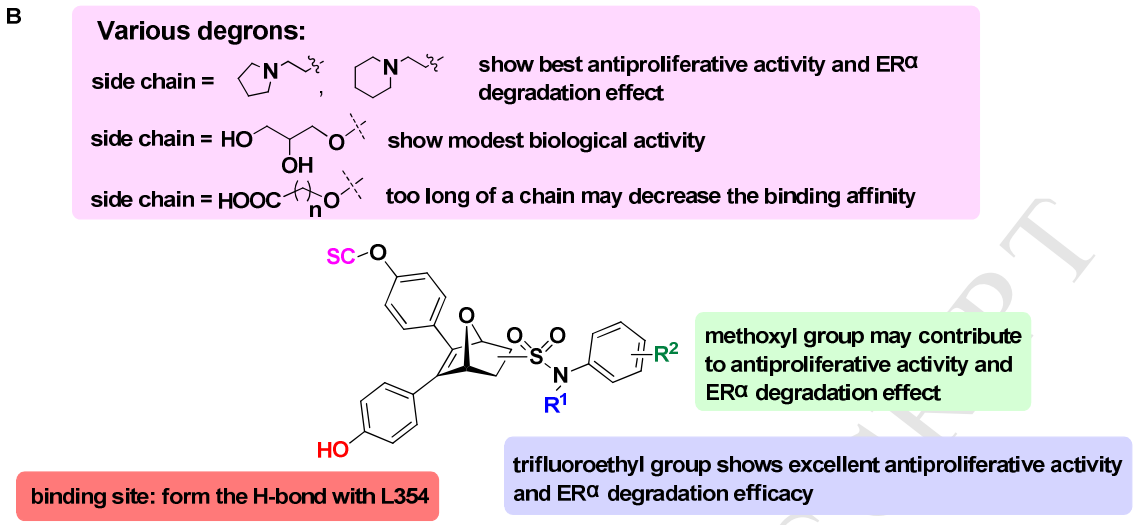

Figure 4. (A) Correlation between the ERα degradation and anti-proliferation activities of different degrons. (B) Structure-activity relationships of the novel SERD compounds.

2.5 Molecular docking

As mentioned above, the obtained compound **17e** turned out to be a single regioisomer, and thus, we analyzed the docking mode of the 2D and 3D interactions between the two enantiomers of compound **17e** and ERα (**Figure 5**). Although we did not obtain another regioisomer **17e'**, we still analyzed the docking mode of the two enantiomers of **17e'** hoping to provide a reference for explaining the biological activity of compound **17e**. The results demonstrated that **17e'** showed less favored interactions with ERα compared to **17e**, and the details are given in the Supporting Information.

In the case of the (1*R*, 2*S*, 4*R*)-enantiomer of compound **17e**, similar to other ER ligands, the phenolic hydroxyl group mimics the A ring of E2 and forms a hydrogen bond with Glu353 on helix 3. At the same time, the basic side chain, as a protein degrading degron, appears to display important interactions with ERα. It forms a hydrogen bond between the nitrogen atom of the basic side chain with Thr347 on helix 3; thus, the entire chain folds in a constrained manner in the binding pocket. In addition, the distance between the *ortho*-methylene group on pyrrolidine and the Met343 is 3.64 Å (Supporting Information), which also develops hydrophobic repulsion with the backbone of Met343 on helix 3 (**Figure 5A, 5B**). These

noncovalent interactions may distort the position of helix 3 so that it could not fold properly, and the ubiquitination of ER will proceed. In contrast, the OBHS analogs with basic side chains published in 2017[45] as ER antagonists formed a hydrogen bond between the basic side chain with Asp351, which stuck out of the pocket toward helix 12. These different interaction modes may illustrate a new mechanism of the basic side chain for degrading ER protein. Moreover, with only a 4.03 Å distance, the *N*-trifluoroethyl substituent demonstrates a hydrophobic interaction with the backbone of Met421 in the loop between helix 7 and helix 8, which is a little different from the crystal structures of **OBHSA** compounds that were reported recently (the *para* substitution on the aryl group would clash with the backbone carbonyl of Glu419 in the loop between helix 7 and helix 8) [38]. For the (1*R*, 2*S*, 4*R*)-enantiomer of compound **17e**, the *para* methoxyl group on the phenyl group is very close to Trp383 and Gly521, which may also clash with the position of helix 11 and thus further enhance the degradation of ERα.

Compared to the (1*R*, 2*S*, 4*R*)-enantiomer, the docking mode of the (1*S*, 2*R*, 4*S*)-enantiomer of compound **17e** is less robust and unstable (**Figure 5C, 5D**). Although the position of the two enantiomers is very similar, there are some differences, which influence their docking mode to ER. The CH_2 group on the basic side chain instead of the nitrogen atom of the (1*R*, 2*S*, 4*R*)-enantiomer interacts with Thr347 but loses the hydrophobic repulsion with the backbone of Met343 on helix 3. Furthermore, the phenolic hydroxyl group of the (1*S*, 2*R*, 4*S*)-configuration failed to form a hydrogen bond with ERα. Although the oxygen atom on the sulfonamide group displays an interaction with Gly521 on helix 11, the (1*S*, 2*R*, 4*S*)-enantiomer displays less interactions than the (1*R*, 2*S*, 4*R*)-enantiomer overall. As a result, only one enantiomer, which possesses the 1*R*, 2*S*, 4*R* absolute configuration, could be docked effectively into the ligand binding pocket, which predicts greater degradation activity for this enantiomer.

From these interaction patterns found in the molecular docking, we can conclude that a new mechanism of the basic side chains on the **OBHSA** scaffold to degrade ER proteins may be discovered, thereby providing the basis for the discovery of new and simpler PROTACs.

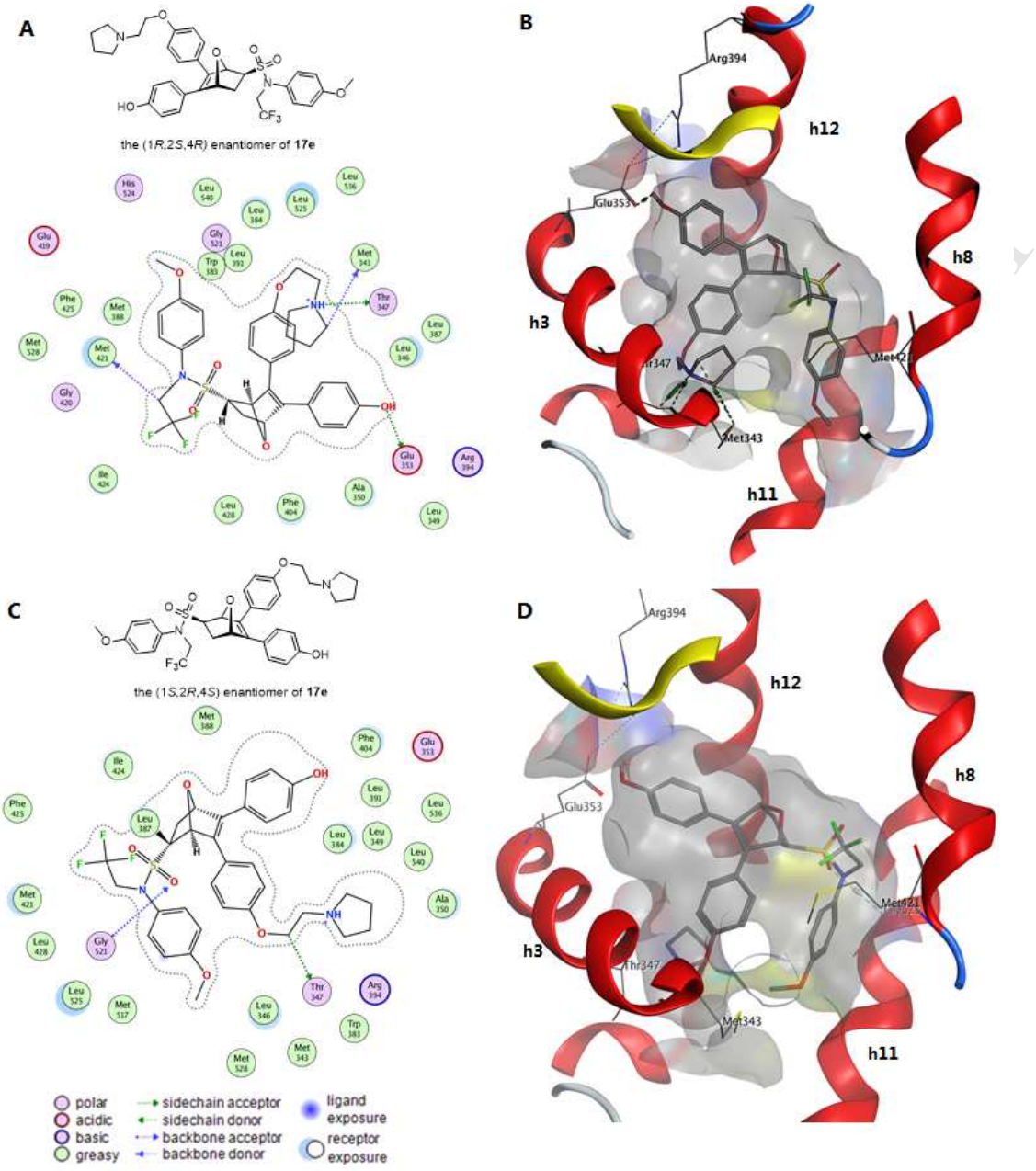

Figure 5. Docking study of two enantiomers of compound **17e** bound to ERα (PDB code: 5kcc). (A) Cartoon schematic of the interactions between the residues of the ERα ligand binding domain with the (1*R*, 2*S*, 4*R*)-enantiomer of compound **17e**. It shows the side chain acceptors of Glu353 and Thr347 in green arrows and the backbone acceptors of Met343 and Met 421 in blue arrows. (B) The docking analysis of the (1*R*, 2*S*, 4*R*)-enantiomer of compound **17e** bound to ERα. The phenolic hydroxyl group forms a hydrogen bond (2.31 Å) with Glu353 on helix 3. The basic side chain forms a hydrogen bond (2.66 Å) between the

nitrogen atom with Thr347, and the ortho-methylene group on pyrrolidine develops hydrophobic repulsion with the backbone of Met343 (3.64 Å) on helix 3. In addition, the *N*-trifluoroethyl substituent demonstrates a hydrophobic interaction with the backbone of Met421 (4.03 Å) in the loop between helix 7 and helix 8. (**C**) Cartoon schematic of the interactions between the residues of the ERα ligand binding domain with the (1*S*, 2*R*, 4*S*)-enantiomer of compound **17e**. It shows the side chain acceptor of Thr347 in a green arrow and the backbone acceptor of Gly521 in a blue arrow. (**D**) The docking analysis of the (1*S*, 2*R*, 4*S*)-enantiomer of compound **17e** bound to ERα. The CH_2 group on the basic side chain develops hydrophobic repulsion with the backbone of Thr347, and the oxygen atom on sulfonamide group displays interaction with the Gly521 on helix 11.

*2.6 Pharmacokinetic profile of **17e** in rats*

Since **17e** showed good cell antiproliferative activity and complete degradation activity, both the oral and intravenous pharmacokinetic profiles of compound **17e** have been investigated, and the results are shown in **Table 3**. Intravenous dosing with a 3 mg/kg solution of **17e** resulted in high clearance (46 mL/min/kg), and the half-lives of *iv* and *po* are 6.2 h and 3.7 h, respectively. The exposure of the compound is good for intravenous injection (1.0 h·μg/mL), while it is moderate by the oral route (0.33 h·μg/mL). The oral bioavailability of **17e** is 9.2%, which is modest compared to other reported SERDs. However, these moderate pharmacokinetic parameters make it possible for further optimal modification of these compounds to improve bioavailability.

Table 3. Pharmacokinetics of **17e** in rats[a]

Administration route	Dose[b] (mg/kg)	CL (mL/min/kg)	$T_{1/2}$ (h)	C_{max} (μg/mL)	AUC (h*μg/mL)	V_{ss} (L/kg)	F (%)
iv	3	46	6.2	1.0	1.08	9.55	
po	10		3.7	0.05	0.33		9.2

[a]Sprague-Dawley rats were used (n = 3). Plasma samples were measured for drug exposure by LC-MS/MS. [b]Dosed intravenously at 3 mg/kg and orally at 10 mg/kg in 5% DMSO and 40% PEG400 in saline.

3. Conclusions

As drug resistance is continuously being identified in the treatment of breast cancer, new strategies based on small molecule-induced protein degradation have developed rapidly. However, most of the candidates involve very limited scaffolds and are still in clinical trials, and none of them has been approved for marketing. Therefore, there is still an urgent need to develop novel compounds with good ER degradation efficacy. In this work, we directed our attention toward discovering new degrons that favor ER degradation and explored the possibility of different side chains (basic side chain, long alkyl acid side chain and glycerol ether side chain) to be the degron of the ER degrader. We designed and synthesized a series of novel **OBHSA** derivatives that contained different side chains and investigated the structure-activity relationships of these compounds. As a result, the basic side chain was confirmed as the appropriate degron because compounds **17d**, **17e** and **17g** with *N*-trifluoroethyl and *para* methoxyl groups exhibited the best anti-proliferative activities and good ERα degradation efficacies. The docking study demonstrates a new mechanism of the basic side chain by forming a hydrogen bond with Thr347 and hydrophobic repulsion with the backbone of Met343, which would distort helix 3. The *N*-trifluoroethyl group and the *para* methoxyl group may also be beneficial to the ERα degradation efficacy by influencing the loop of helix 7 and helix 8. Although these compounds showed micromolar activities and modest oral bioavailability, the novel skeleton and easy modification of these PROTAC-like SERDs allow further fine-tuning of their pharmacokinetic properties including oral availability. In summary, these findings simplified the structure of currently available degrons and provide new possibilities for discovering novel scaffolds in the development of novel PROTACs.

4. Experimental section

4.1 General chemical methods.

Starting materials, reagents and solvents are purchased from commercial sources and used directly unless otherwise noted. THF, DCM and acetonitrile are redistilled and dried to avoid

water. Glassware was oven-dried, assembled while hot, and cooled under an inert atmosphere. Reaction progress was monitored using analytical thin-layer chromatography (TLC). Visualization was achieved by UV light (254 nm and 365 nm). Silica gel (230−400 mesh) was used for column chromatography purifications. A Bruker Biospin AV400 (400 MHz, ^{1}H NMR; 100 MHz, ^{13}C NMR) instrument was used to measure the ^{1}H NMR and ^{13}C NMR spectra.

The synthesis of intermediate compounds **8a**-**j**, **15**, **16a**-**h** is reported in the Supporting Information.

4.2 Chemistry.

*4.2.1 General procedure for the synthesis of final compounds**17a-t***

We used the distilled THF (2 mL) as cosolvent and added furans **8a**-**d** or **8h**-**j** (0.6 mmol) and dienophiles **14a** or **14c**-**f** (0.6 mmol) to the round-bottom flask. The reaction mixture was heated to 90 °C and stirred for 8 h under argon. The crude product was purified by silica gel column chromatography (DCM-MeOH, 50:1-20:1).

*4.2.2 Characterization data for final compounds **17a-t***

*6-(4-(2,3-Dihydroxypropoxy)phenyl)-N-ethyl-5-(4-hydroxyphenyl)-N-phenyl-7-oxabicyclo[2.2.1]hept-5-ene-2-sulfonamide (**17a**)*: Yellow solid, 61% yield, mp 96-98 °C. ^{1}H NMR (400 MHz, MeOD) δ 7.34 – 7.27 (m, 5H), 7.24 – 7.16 (m, 2H), 7.12 (dt, *J* = 14.9, 7.5 Hz, 2H), 6.88 (dd, *J* = 17.1, 8.7 Hz, 2H), 6.73 (dd, *J* = 18.5, 8.6 Hz, 2H), 5.44 (d, *J* = 10.7 Hz, 1H), 5.28 (t, *J* = 3.8 Hz, 1H), 4.08 – 4.02 (m, 1H), 4.02 – 3.95 (m, 2H), 3.84 – 3.75 (m, 2H), 3.67 (ddd, *J* = 12.3, 10.2, 5.0 Hz, 2H), 3.46 (td, *J* = 8.4, 4.5 Hz, 1H), 2.20 (dd, *J* = 7.6, 4.5 Hz, 1H), 1.99 (s, 1H), 1.04 (t, *J* = 7.0 Hz, 3H). ^{13}C NMR (101 MHz, MeOD) δ 158.76, 157.50, 141.54, 140.51, 138.82, 137.70, 136.65, 129.06, 128.97, 128.94, 128.76, 128.35, 128.16, 127.65, 125.39, 123.08, 115.43, 114.42, 84.41, 82.72, 70.37, 68.97, 62.79, 60.20, 46.39, 19.57, 13.61. HRMS (ESI) calcd for $C_{29}H_{31}NO_7S$ $[M + H]^+$, 560.1713; found 560.1713.

*6-(4-(2,3-Dihydroxypropoxy)phenyl)-5-(4-hydroxyphenyl)-N-(4-methoxyphenyl)-N-(2,2,2-trifluoroethyl)-7-oxabicyclo[2.2.1]hept-5-ene-2-sulfonamide (**17b**, Mixture of 4:1 Isomers)*: Yellow solid, 74% yield, mp 99-100 °C. ^{1}H NMR (400 MHz, MeOD) δ 7.32 – 7.18 (m, 4H), 7.18 – 7.08 (m, 2H), 7.00 – 6.90 (m, 2H), 6.87 (d, *J* = 8.8 Hz, 1H), 6.83 – 6.78 (m, 2H), 6.73 – 6.68 (m, 1H), 5.47 (d, *J* = 5.3 Hz, 1H), 5.31 (s, 1H), 4.42 (q, *J* = 8.5 Hz, 2H), 4.08 – 4.03 (m, 1H), 4.02 – 3.95 (m, 2H), 3.78 (s, 3H), 3.73 – 3.65 (m, 2H), 3.51 – 3.42 (m, 1H), 2.28 – 2.19 (m, 1H), 2.09 – 2.03 (m, 1H). ^{13}C NMR (101 MHz, MeOD) δ 159.66, 159.01, 158.79, 157.64, 157.38, 141.75, 140.71, 137.61, 136.46, 131.36, 130.15, 129.24, 129.01, 128.18, 127.98, 125.32, 124.61, 124.16 (d, $^{1}J_{CF}$ = 279.6 Hz), 123.63, 122.98, 115.43, 115.14, 114.64, 114.37, 114.18, 84.40, 84.25, 82.70, 82.65, 70.36, 69.04, 68.95, 62.73, 61.14 (d, $^{2}J_{CF}$ = 30.9 Hz), 60.16, 54.61, 54.56, 53.42, 51.93, 22.35, 19.49. HRMS (ESI) calcd for $C_{30}H_{30}F_3NO_8S$ [M + Na]$^{+}$, 644.1536; found 644.1531.

*N-(4-Chlorophenyl)-6-(4-(2,3-dihydroxypropoxy)phenyl)-5-(4-hydroxyphenyl)-N-(2,2,2-trifluoroethyl)-7-oxabicyclo[2.2.1]hept-5-ene-2-sulfonamide(**17c**)*: Yellow solid, 56% yield, mp 95-97 °C. ^{1}H NMR (400 MHz, MeOD) δ 7.42 – 7.26 (m, 4H), 7.21 (dd, *J* = 12.8, 6.1 Hz, 2H), 7.17 – 7.08 (m, 2H), 6.98 – 6.86 (m, 2H), 6.81 – 6.69 (m, 2H), 5.45 (d, *J* = 18.9 Hz, 1H), 5.32 (s, 1H), 4.50 (dd, *J* = 16.3, 8.1 Hz, 2H), 4.06 (dd, *J* = 12.5, 7.5 Hz, 1H), 4.03 – 3.94 (m, 2H), 3.69 (dd, *J* = 11.2, 4.9 Hz, 2H), 3.50 (d, *J* = 7.8 Hz, 1H), 2.22 – 2.13 (m, 1H), 2.03 (s, 1H). ^{13}C NMR (101 MHz, MeOD) δ 159.02, 157.42, 140.79, 137.96, 136.37, 134.01, 130.20, 129.23, 129.11, 128.23, 124.06 (d, $^{1}J_{CF}$ = 280.3 Hz), 115.41, 115.14, 114.63, 114.37, 84.38, 82.73, 70.36, 69.02, 68.94, 62.19(d, $^{2}J_{CF}$ = 32.9 Hz), 62.02, 61.83, 60.16, 30.18, 19.48. HRMS (ESI) calcd for $C_{29}H_{27}ClF_3NO_7S$ [M + Na]+, 648.1041; found 648.1038.

*6-(4-(2-(Dimethylamino)ethoxy)phenyl)-5-(4-hydroxyphenyl)-N-(4-methoxyphenyl)-N-(2,2,2-trifluoroethyl)-7-oxabicyclo[2.2.1]hept-5-ene-2-sulfonamide (**17d**, Mixture of 5:1 Isomers)*: Yellow solid, 75% yield, mp 99-101 °C. ^{1}H NMR (400 MHz, MeOD) δ 7.29 – 7.20 (m, 4H), 7.13 (dd, *J* = 8.6, 7.2 Hz, 2H), 6.97 (d, *J* = 8.7 Hz, 1H), 6.92 (d, *J* = 8.8 Hz, 1H), 6.84 (d, *J* = 9.0 Hz, 1H), 6.82 – 6.75 (m, 2H), 6.71 (d, *J* = 8.6 Hz, 1H), 5.48 (s, 1H), 5.32 (dd, *J* = 7.0, 4.1 Hz, 1H), 4.42 (dd, *J* = 16.9, 8.5 Hz, 2H), 4.27 (dt, *J* = 12.8, 4.6 Hz, 2H), 3.78 (d, *J* = 2.9 Hz,

3H), 3.47 (ddd, *J* = 17.7, 8.3, 4.4 Hz, 1H), 3.29 (t, *J* = 5.9 Hz, 2H), 2.75 (t, *J* = 4.8 Hz, 6H), 2.27 – 2.19 (m, 1H), 2.07 – 2.03 (m, 1H). ^{13}C NMR (101 MHz, MeOD) δ 159.68, 158.01, 157.81, 157.76, 157.51, 142.16, 140.61, 137.98, 136.31, 131.42, 131.30, 130.16, 129.27, 128.99, 128.25, 128.08, 126.04, 124.15(d, $^{1}J_{CF}$ = 280.0 Hz), 123.48, 115.47, 115.18, 114.68, 114.44, 114.31, 114.18, 113.79, 84.41, 84.36, 82.76, 82.62, 63.14, 61.46, 61.21 (d, $^{2}J_{CF}$ = 30.7 Hz), 61.03, 60.15, 56.71, 54.57, 43.21, 30.10, 29.39, 21.25, 19.49.HRMS (ESI) calcd for $C_{31}H_{33}F_3N_2O_6S$ $[M + Na]^+$, 642.1937; found 642.1928.

*5-(4-Hydroxyphenyl)-N-(4-methoxyphenyl)-6-(4-(2-(pyrrolidin-1-yl)ethoxy)phenyl)-N-(2,2,2-trifluoroethyl)-7-oxabicyclo[2.2.1]hept-5-ene-2-sulfonamide (**17e**)*: Yellow solid, 72% yield, mp 115-117 °C. ^{1}H NMR (400 MHz, MeOD) δ 7.45 – 7.34 (m, 1H), 7.35 – 7.17 (m, 4H), 7.18 – 7.08 (m, 2H), 7.00 – 6.91 (m, 2H), 6.83 (dd, *J* = 12.6, 3.6 Hz, 1H), 6.79 (dd, *J* = 8.7, 5.0 Hz, 1H), 6.71 (dd, *J* = 8.5, 3.7 Hz, 1H), 5.49 (d, *J* = 8.1 Hz, 1H), 5.30 (dd, *J* = 10.1, 4.0 Hz, 1H), 4.48 – 4.34 (m, 2H), 4.29 (dt, *J* = 10.0, 5.1 Hz, 2H), 3.78 (dd, *J* = 14.8, 2.8 Hz, 3H), 3.52 (dd, *J* = 10.2, 5.7 Hz, 2H), 3.49 – 3.43 (m, 1H), 3.32 (dd, *J* = 4.6, 3.0 Hz, 4H), 2.29 – 2.16 (m, 1H), 2.10 – 2.04 (m, 4H), 2.04 – 1.99 (m, 1H). ^{13}C NMR (101 MHz, MeOD) δ 159.68, 157.89, 157.07, 140.10, 138.01, 131.40, 130.18, 129.45, 129.03, 128.30, 124.24 (d, $^{1}J_{CF}$ = 282.1 Hz), 115.51, 115.23, 114.54, 114.24, 84.43, 82.78, 63.76, 61.32 (d, $^{2}J_{CF}$ = 31.8 Hz), 61.06, 54.67, 54.30, 53.89, 30.15, 22.61. HRMS (ESI) calcd for $C_{33}H_{35}F_3N_2O_6S$ $[M + Na]^+$, 667.2060; found 667.2047.

*5-(4-Hydroxyphenyl)-6-(4-(2-(piperidin-1-yl)ethoxy)phenyl)-N-(p-tolyl)-N-(2,2,2-trifluoroethyl)-7-oxabicyclo[2.2.1]hept-5-ene-2-sulfonamide (**17f**,* Mixture of 4:1 Isomers*)*: Yellow solid, 81% yield, mp 101-103 °C. ^{1}H NMR (400 MHz, MeOD) δ 7.27 – 7.18 (m, 4H), 7.12 (d, *J* = 8.2 Hz, 2H), 6.97 – 6.91 (m, 1H), 6.88 (d, *J* = 8.7 Hz, 1H), 6.80 – 6.74 (m, 1H), 6.71 (d, *J* = 8.5 Hz, 1H), 5.47 (d, *J* = 3.7 Hz, 1H), 5.31 (t, *J* = 3.9 Hz, 1H), 4.45 (dd, *J* = 17.0, 8.5 Hz, 2H), 4.19 (dt, *J* = 16.8, 5.3 Hz, 2H), 3.47 (ddd, *J* = 12.9, 8.3, 4.3 Hz, 1H), 2.97 (dt, *J* = 16.2, 5.7 Hz, 2H), 2.76 (s, 4H), 2.35 (d, *J* = 18.9 Hz, 3H), 2.23 – 2.16 (m, 1H), 2.02 (dd, *J* = 13.7, 4.3 Hz, 1H), 1.71 (dd, *J* = 10.5, 5.3 Hz, 4H), 1.55 (s, 2H). ^{13}C NMR (101 MHz, MeOD) δ 158.52, 158.37, 157.69, 157.52, 138.59, 137.76, 137.25, 136.53, 136.44, 136.38, 130.00, 129.81,

129.70, 129.15, 129.04, 128.94, 128.51, 128.25, 128.08, 125.52, 124.24 (d, $^{1}J_{CF}$ = 281.1 Hz), 123.53, 123.05, 115.43, 115.19, 114.62, 114.40, 84.38, 84.35, 82.73, 82.63, 64.07, 63.96, 61.49, 61.45 (d, $^{2}J_{CF}$ = 31.2 Hz), 60.15, 56.93, 56.89, 54.18, 53.44, 30.17, 29.40, 24.32, 24.27, 22.86, 22.82, 19.75, 19.71. HRMS (ESI) calcd for $C_{34}H_{37}F_3N_2O_5S$ $[M + H]^+$, 643.2448; found 643.2456.

*5-(4-Hydroxyphenyl)-N-(4-methoxyphenyl)-6-(4-(2-(piperidin-1-yl)ethoxy)phenyl)-N-(2,2,2-trifluoroethyl)-7-oxabicyclo[2.2.1]hept-5-ene-2-sulfonamide (**17g**, Mixture of 3:1 Isomers)*: Yellow solid, 75% yield, mp 106-108 °C. ^{1}H NMR (400 MHz, MeOD) δ 7.27 – 7.19 (m, 4H), 7.13 (t, *J* = 8.6 Hz, 2H), 6.93 (d, *J* = 8.8 Hz, 1H), 6.90 – 6.82 (m, 2H), 6.79 (dd, *J* = 8.7, 4.7 Hz, 2H), 6.71 (d, *J* = 8.6 Hz, 1H), 5.48 (s, 1H), 5.31 (t, *J* = 3.7 Hz, 1H), 4.42 (dd, *J* = 17.0, 8.4 Hz, 2H), 4.17 (dd, *J* = 11.5, 5.5 Hz, 2H), 3.81 – 3.75 (m, 3H), 3.51 – 3.42 (m, 1H), 2.92 (dt, *J* = 10.5, 5.3 Hz, 2H), 2.70 (s, 4H), 2.23 (ddd, *J* = 11.2, 7.6, 4.3 Hz, 1H), 2.01 (dd, *J* = 8.3, 4.1 Hz, 1H), 1.69 (dd, *J* = 10.3, 5.1 Hz, 5H), 1.53 (s, 2H). ^{13}C NMR (101 MHz, MeOD) δ 159.65, 158.53, 158.31, 157.68, 157.42, 141.84, 140.65, 137.62, 136.37, 131.35, 131.27, 130.16, 129.50, 129.27, 129.03, 128.21, 128.03, 125.46, 124.15 (d, $^{1}J_{CF}$ = 279.9 Hz), 122.89, 115.47, 115.17, 114.61, 114.35, 114.18, 84.36, 84.21, 83.05, 82.63, 64.43, 64.35, 61.16 (d, $^{2}J_{CF}$ = 28.9 Hz), 60.20, 57.14, 54.58, 54.31, 54.17, 53.44, 52.29, 51.94, 31.36, 30.21, 28.73, 24.63, 24.39, 23.16. HRMS (ESI) calcd for $C_{34}H_{37}F_3N_2O_6S$ $[M + Na]^+$, 681.2217; found 681.2217.

*5-(4-Hydroxyphenyl)-N-methyl-N-phenyl-6-(4-(2-(piperidin-1-yl)ethoxy)phenyl)-7-oxabicyclo[2.2.1]hept-5-ene-2-sulfonamide (**17h**)*: Yellow solid, 70% yield, mp 96-98 °C. ^{1}H NMR (400 MHz, MeOD) δ 7.48 – 7.44 (m, 1H), 7.40 – 7.33 (m, 4H), 7.26 – 7.20 (m, 2H), 7.16 – 7.08 (m, 2H), 6.92 (dd, *J* = 13.2, 8.9 Hz, 2H), 6.78 – 6.69 (m, 2H), 5.43 (s, 1H), 5.33 – 5.27 (m, 1H), 4.24 (dt, *J* = 10.8, 5.3 Hz, 2H), 3.53 (td, *J* = 8.7, 4.4 Hz, 1H), 3.37 (t, *J* = 5.6 Hz, 3H), 3.16 – 3.06 (m, 2H), 2.89 (s, 4H), 2.21 (d, *J* = 7.4 Hz, 1H), 2.19 – 2.15 (m, 1H), 1.75 (dt, *J* = 10.7, 5.4 Hz, 4H), 1.59 (s, 4H), 0.92 (t, *J* = 6.8 Hz, 2H). ^{13}C NMR (101 MHz, MeOD) δ 158.49, 157.44, 141.69, 137.72, 129.40, 128.84, 128.52 (dd, *J* = 42.1, 15.4 Hz), 126.97, 126.48, 124.90, 123.62, 115.36, 115.17, 114.54, 114.36, 84.31, 82.77, 64.64, 60.55, 60.15, 57.29, 54.39, 38.07, 24.77, 23.33, 19.49. HRMS (ESI) calcd for $C_{32}H_{36}N_2O_5S$ $[M + H]^+$, 561.2418;

found 561.2418.

*N-Ethyl-5-(4-hydroxyphenyl)-N-phenyl-6-(4-(2-(piperidin-1-yl)ethoxy)phenyl)-7-oxabicyclo[2.2.1]hept-5-ene-2-sulfonamide (**17i**)*: Yellow solid, 72% yield, mp 97-100 °C. ^{1}H NMR (400 MHz, MeOD) δ 7.32 (dd, *J* = 8.4, 6.3 Hz, 4H), 7.26 – 7.19 (m, 2H), 7.18 – 7.07 (m, 2H), 6.93 – 6.84 (m, 2H), 6.74 (dd, *J* = 19.6, 8.6 Hz, 2H), 5.46 (s, 1H), 5.30 (t, *J* = 3.1 Hz, 1H), 4.14 (dt, *J* = 9.1, 5.5 Hz, 2H), 3.80 (dt, *J* = 17.5, 7.1 Hz, 2H), 3.52 – 3.43 (m, 1H), 2.82 (dt, *J* = 7.9, 5.2 Hz, 2H), 2.61 (s, 4H), 2.27 – 2.14 (m, 1H), 2.03 (ddd, *J* = 14.0, 8.5, 3.8 Hz, 1H), 1.66 (dd, *J* = 9.5, 5.0 Hz, 4H), 1.51 (s, 2H), 1.09 – 1.03 (m, 3H). ^{13}C NMR (101 MHz, MeOD) δ 158.60, 157.42, 141.58, 138.84, 136.59, 129.05, 128.90, 128.77, 128.31, 128.16, 127.63, 125.44, 123.68, 115.18, 114.56, 84.40, 82.77, 64.85, 61.35, 60.17, 57.40, 54.50, 46.34, 24.92, 23.49, 19.50, 13.55. HRMS (ESI) calcd for $C_{33}H_{38}N_2O_5S$ $[M + Na]^+$, 597.2394; found 597.2398.

*7-(4-(6-(N-Ethyl-N-phenylsulfamoyl)-3-(4-hydroxyphenyl)-7-oxabicyclo[2.2.1]hept-2-en-2-yl) phenoxy)heptanoic acid (**17j**, Mixture of 3:1 Isomers)*: Yellow solid, 60% yield, mp 103-105 °C. ^{1}H NMR (400 MHz, Acetone-d_6) δ 7.47 – 7.41 (m, 1H), 7.40 – 7.33 (m, 4H), 7.27 (d, *J* = 8.8 Hz, 2H), 7.23 – 7.15 (m, 2H), 6.90 (dd, *J* = 14.5, 8.8 Hz, 2H), 6.85 – 6.79 (m, 2H), 5.49 (s, 1H), 5.36 – 5.31 (m, 1H), 4.04 – 3.98 (m, 2H), 3.92 – 3.80 (m, 2H), 3.53 (ddd, *J* = 7.6, 4.3, 3.0 Hz, 1H), 2.33 (dd, J = 10.2, 4.5 Hz, 2H), 2.18 (tt, *J* = 11.3, 5.7 Hz, 1H), 2.09 (dd, *J* = 7.7, 4.5 Hz, 1H), 1.84 – 1.76 (m, 2H), 1.68 – 1.61 (m, 2H), 1.52 (dd, *J* = 17.5, 10.7 Hz, 2H), 1.48 – 1.41 (m, 2H), 1.08 – 0.98 (m, 3H). ^{13}C NMR (101 MHz, MeOD) δ176.31, 159.13, 158.98, 157.53, 157.35, 141.33, 140.54, 138.84, 137.50, 131.66, 131.41, 129.06, 128.89, 128.72, 128.27, 128.09, 127.62, 125.00, 124.37, 123.76, 123.10, 115.35, 115.12, 114.74, 114.48, 114.25, 113.74, 84.37, 84.13, 83.18, 82.77, 67.53, 67.47, 61.31, 61.19, 60.65, 60.15, 59.66, 46.35, 33.49, 28.79, 28.58, 25.47, 24.63, 19.48, 13.54, 13.37. HRMS (ESI) calcd for $C_{33}H_{37}NO_7S$ $[M + Na]^+$, 614.2183; found 614.2184.

*8-(4-(6-(N-Ethyl-N-phenylsulfamoyl)-3-(4-hydroxyphenyl)-7-oxabicyclo[2.2.1]hept-2-en-2-yl) phenoxy)octanoic acid (**17k**)*: Yellow solid, 63% yield, mp 88-90 °C. ^{1}H NMR (400 MHz, Acetone-d_6) δ 7.41 – 7.34 (m, 4H), 7.27 (d, *J* = 8.7 Hz, 2H), 7.19 (dd, *J* = 10.6, 9.4 Hz, 2H), 6.90 (dd, *J* = 14.5, 8.8 Hz, 2H), 6.81 (dt, *J* = 17.3, 7.3 Hz, 2H), 5.49 (s, 1H), 5.34 (d, *J* = 4.1

Hz, 1H), 4.02 (dt, *J* = 10.1, 6.5 Hz, 2H), 3.86 (q, *J* = 7.0 Hz, 2H), 3.57 – 3.50 (m, 1H), 2.31 (t, *J* = 7.4 Hz, 2H), 2.23 – 2.13 (m, 1H), 2.10 – 2.07 (m, 1H), 1.79 (dq, *J* = 13.0, 6.3 Hz, 2H), 1.69 – 1.58 (m, 2H), 1.56 – 1.47 (m, 2H), 1.42 (t, *J* = 11.9 Hz, 4H), 1.04 (dd, *J* = 14.3, 7.2 Hz, 3H). ^{13}C NMR (101 MHz, MeOD) δ 176.35, 158.98, 157.33, 141.33, 138.85, 136.71, 129.05, 128.90, 128.73, 128.31, 128.12, 127.62, 124.98, 123.13, 115.40, 114.52, 84.38, 82.71, 67.63, 61.40, 46.37, 33.54, 30.12, 28.89, 28.77, 25.60, 24.64, 13.58. HRMS (ESI) calcd for $C_{34}H_{39}NO_7S$ $[M + Na]^+$, 628.2339; found 628.2336.

*11-(4-(6-(N-Ethyl-N-phenylsulfamoyl)-3-(4-hydroxyphenyl)-7-oxabicyclo[2.2.1]hept-2-en-2-yl)phenoxy)undecanoic acid (**17l**)*: Yellow solid, 69% yield, mp 80-82 °C. ^{1}H NMR (400 MHz, Acetone-d_6) δ 7.39 – 7.32 (m, 4H), 7.30 – 7.24 (m, 2H), 7.19 (dt, *J* = 14.0, 6.0 Hz, 2H), 6.91 (dt, *J* = 11.6, 8.5 Hz, 2H), 6.85 – 6.75 (m, 2H), 5.50 (d, *J* = 4.2 Hz, 1H), 5.38 – 5.31 (m, 1H), 4.00 (dt, *J* = 14.0, 5.6 Hz, 2H), 3.86 (q, *J* = 7.1 Hz, 2H), 3.59 – 3.49 (m, 1H), 2.29 (t, *J* = 7.4 Hz, 2H), 2.19 (dt, *J* = 11.9, 4.4 Hz, 1H), 2.08 (dd, *J* = 4.8, 2.6 Hz, 1H), 1.78 (tt, *J* = 12.9, 6.4 Hz, 2H), 1.59 (dd, *J* = 13.8, 6.8 Hz, 2H), 1.49 (dd, *J* = 11.0, 5.8 Hz, 2H), 1.34 (s, 10H), 1.10 – 1.01 (m, 3H). ^{13}C NMR (101 MHz, MeOD) δ 171.63, 159.66, 157.53, 140.62, 136.27, 131.38, 130.16, 129.28, 129.02, 128.24, 128.06, 123.50, 122.82, 115.45, 115.15, 114.39, 114.16, 84.35, 82.62, 65.70, 61.38, 54.55, 53.96, 30.17, 29.39, 23.85, 22.43, 21.26, 20.66, 13.08. HRMS (ESI) calcd for $C_{37}H_{45}NO_7S$ $[M + Na]^+$, 670.2809; found 670.2798.

*7-(4-(3-(4-Hydroxyphenyl)-6-(N-(4-methoxyphenyl)-N-(2,2,2-trifluoroethyl)sulfamoyl)-7-oxabicyclo[2.2.1]hept-2-en-2-yl)phenoxy)heptanoic acid (**17m**)*: Yellow solid, 68% yield, mp 94-97 °C. ^{1}H NMR (400 MHz, Acetone-d_6) δ 7.38 – 7.32 (m, 2H), 7.27 (t, *J* = 8.4 Hz, 2H), 7.21 (t, *J* = 9.0 Hz, 2H), 6.94 (d, *J* = 8.7 Hz, 1H), 6.91 – 6.83 (m, 4H), 6.81 (t, J = 7.7 Hz, 1H), 5.56 (d, *J* = 1.4 Hz, 1H), 5.36 (s, 1H), 4.52 (q, *J* = 8.6 Hz, 2H), 4.03 (ddd, *J* = 16.0, 9.6, 4.7 Hz, 2H), 3.82 (d, *J* = 13.0 Hz, 3H), 3.58 (dt, *J* = 8.2, 4.1 Hz, 1H), 2.33 (td, *J* = 7.3, 3.2 Hz, 2H), 2.25 – 2.16 (m, 1H), 2.12 – 2.08 (m, 1H), 1.85 – 1.74 (m, 2H), 1.70 – 1.59 (m, 2H), 1.56 – 1.39 (m, 4H). ^{13}C NMR (101 MHz, Acetone-d_6) δ 173.88, 159.45, 159.14, 157.55, 141.65, 137.73, 131.87, 130.40, 129.33, 129.15, 128.34, 125.82, 124.42 (d, $^1J_{CF}$ = 280.0 Hz), 115.71, 115.49, 114.72, 114.51, 114.30, 84.32, 82.67, 67.65, 67.58, 61.72, 54.89, 33.23, 30.47, 28.95,

28.68, 25.63, 24.70. HRMS (ESI) calcd for $C_{34}H_{36}F_3NO_8S$ $[M + Na]^+$, 698.2006; found 698.2002.

*8-(4-(3-(4-Hydroxyphenyl)-6-(N-(4-methoxyphenyl)-N-(2,2,2-trifluoroethyl)sulfamoyl)-7-oxabicyclo[2.2.1]hept-2-en-2-yl)phenoxy)octanoic acid (**17n**)*: Yellow solid, 70% yield, mp 91-94 °C. ^{1}H NMR (400 MHz, Acetone-d_6) δ 8.99 – 8.44 (m, 1H), 7.39 – 7.31 (m, 2H), 7.26 (dt, *J* = 15.7, 7.8 Hz, 2H), 7.19 (dd, *J* = 16.6, 8.2 Hz, 2H), 6.93 (t, *J* = 8.2 Hz, 1H), 6.91 – 6.83 (m, 4H), 6.82 – 6.76 (m, 1H), 5.65 – 5.48 (m, 1H), 5.36 (d, *J* = 2.9 Hz, 1H), 4.60 – 4.46 (m, 2H), 4.05 – 3.98 (m, 2H), 3.81 (s, 3H), 3.62 – 3.51 (m, 1H), 2.31 (td, *J* = 7.4, 2.3 Hz, 2H), 2.19 (ddd, *J* = 15.4, 10.2, 5.3 Hz, 1H), 2.13 – 2.08 (m, 1H), 1.85 – 1.76 (m, 2H), 1.66 – 1.58 (m, 2H), 1.55 – 1.47 (m, 2H), 1.42 (t, *J* = 6.6 Hz, 4H). ^{13}C NMR (101 MHz, Acetone-d_6) δ 173.80, 159.52, 159.15, 157.53, 131.88, 130.39, 129.31, 128.33, 125.20, 124.42 (d, $^1J_{CF}$ = 280.3 Hz), 123.45, 115.70, 115.48, 114.71, 114.51, 114.29, 84.34, 82.70, 67.63, 61.71, 59.67, 54.88, 33.27, 30.43, 28.88, 25.72, 24.71, 19.94, 13.61. HRMS (ESI) calcd for $C_{35}H_{38}F_3NO_8S$ $[M + Na]^+$, 712.2162; found 712.2167.

*11-(4-(3-(4-Hydroxyphenyl)-6-(N-(4-methoxyphenyl)-N-(2,2,2-trifluoroethyl)sulfamoyl)-7-oxabicyclo[2.2.1]hept-2-en-2-yl)phenoxy)undecanoic acid (**17o**)*: Yellow solid, 59% yield, mp 81-83 °C. ^{1}H NMR (400 MHz, Acetone-d_6) δ 7.39 – 7.31 (m, 2H), 7.31 – 7.24 (m, 2H), 7.19 (dd, *J* = 16.6, 8.2 Hz, 2H), 6.96 – 6.78 (m, 6H), 5.55 (d, *J* = 0.9 Hz, 1H), 5.36 (d, *J* = 3.2 Hz, 1H), 4.64 – 4.37 (m, 2H), 4.05 – 3.97 (m, 2H), 3.80 (s, 3H), 3.60 – 3.53 (m, 1H), 2.29 (t, *J* = 7.4 Hz, 2H), 2.20 (dt, *J* = 11.9, 4.4 Hz, 1H), 2.12 – 2.08 (m, 1H), 1.84 – 1.73 (m, 2H), 1.63 – 1.57 (m, 2H), 1.49 (dd, *J* = 15.3, 8.0 Hz, 2H), 1.34 (s, 10H). ^{13}C NMR (101 MHz, Acetone-d_6) δ 173.85, 159.45, 158.99, 157.58, 140.97, 137.73, 131.86, 130.39, 129.32, 128.33, 125.19, 124.42 (d, $^1J_{CF}$ = 280.1 Hz), 123.45, 115.70, 115.48, 114.70, 114.29, 84.33, 82.66, 67.72, 67.65, 61.83 (d, $^2J_{CF}$ = 25.2 Hz), 61.62, 54.88, 33.31, 30.47, 25.86, 24.77. HRMS (ESI) calcd for $C_{38}H_{44}F_3NO_8S$ $[M + Na]^+$, 754.2632; found 754.2633.

*N-(4-(2,3-Dihydroxypropoxy)phenyl)-N-ethyl-5,6-bis(4-hydroxyphenyl)-7-oxabicyclo[2.2.1]hept-5-ene-2-sulfonamide (**17p**)*: Yellow solid, 76% yield, mp 126-128 °C. ^{1}H NMR (400 MHz, Acetone-d_6) δ 7.27 (t, *J* = 7.4 Hz, 3H), 7.20 (d, *J* = 8.5 Hz, 4H), 6.90 (d, *J* = 8.8 Hz, 2H), 6.82

(dd, *J* = 16.8, 8.5 Hz, 4H), 5.46 (s, 1H), 5.32 (t, *J* = 4.6 Hz, 1H), 4.20 (s, 1H), 4.00 (t, *J* = 5.8 Hz, 2H), 3.90 (s, 1H), 3.79 (q, *J* = 7.0 Hz, 2H), 3.69 (s, 2H), 3.48 (dd, *J* = 8.3, 4.5 Hz, 1H), 2.21 (dt, *J* = 11.8, 4.4 Hz, 1H), 2.10 – 2.07 (m, 1H), 1.04 (t, *J* = 7.1 Hz, 3H). ^{13}C NMR (101 MHz, Acetone-d_6) δ 158.38, 157.28, 140.89, 137.50, 131.75, 130.57, 129.09, 128.50, 124.43, 115.67, 115.45, 114.65, 84.45, 82.69, 70.41, 69.57, 63.13, 61.29, 46.34, 19.97, 14.02. HRMS (ESI) calcd for $C_{29}H_{31}NO_8S$ $[M + Na]^+$, 576.1663; found 576.1662.

*N-Ethyl-5,6-bis(4-hydroxyphenyl)-N-(4-(2-(piperidin-1-yl)ethoxy)phenyl)-7-oxabicyclo[2.2.1] hept-5-ene-2-sulfonamide (**17q**)*: Yellow solid, 78% yield, mp 123-125 °C. ^{1}H NMR (400 MHz, Acetone-d_6) δ 7.22 (d, *J* = 8.8 Hz, 2H), 7.17 (dd, *J* = 15.1, 8.6 Hz, 4H), 6.87 (dd, *J* = 15.9, 7.8 Hz, 4H), 6.80 (d, *J* = 8.6 Hz, 2H), 5.42 (d, *J* = 5.5 Hz, 1H), 5.33 (d, *J* = 4.1 Hz, 1H), 4.36 – 4.23 (m, 2H), 3.85 – 3.71 (m, 2H), 3.44 (ddd, *J* = 12.8, 8.5, 4.4 Hz, 1H), 3.10 (dt, *J* = 11.0, 5.5 Hz, 2H), 2.98 – 2.79 (m, 4H), 2.31 – 2.19 (m, 1H), 2.15 – 2.08 (m, 1H), 1.73 (dt, *J* = 11.2, 5.6 Hz, 4H), 1.53 (d, *J* = 4.8 Hz, 2H), 1.03 (t, *J* = 7.0 Hz, 3H). ^{13}C NMR (101 MHz, Acetone-d_6) δ 157.69, 157.24, 140.79, 137.46, 131.96, 130.41, 129.21, 128.38, 124.31, 123.55, 115.72, 115.40, 114.72, 84.61, 82.57, 64.70, 60.92, 56.78, 54.16, 46.24, 24.48, 23.04, 19.98, 14.07. HRMS (ESI) calcd for $C_{33}H_{38}N_2O_6S$ $[M + Na]^+$, 613.2343; found 613.2348.

*7-(4-(N-Ethyl-5,6-bis(4-hydroxyphenyl)-7-oxabicyclo[2.2.1]hept-5-ene-2-sulfonamido)pheno xy)heptanoic acid (**17r**)*: Yellow solid, 73% yield, mp 105-106 °C. ^{1}H NMR (400 MHz, Acetone-d_6) δ 7.33 – 7.24 (m, 2H), 7.24 – 7.17 (m, 4H), 6.85 (dt, *J* = 13.8, 7.0 Hz, 4H), 6.80 (d, *J* = 8.6 Hz, 2H), 5.48 (s, 1H), 5.33 (d, *J* = 3.9 Hz, 1H), 3.99 (t, *J* = 6.4 Hz, 2H), 3.78 (q, *J* = 7.0 Hz, 2H), 3.48 (dd, *J* = 8.3, 4.4 Hz, 1H), 2.32 (t, *J* = 7.3 Hz, 2H), 2.20 (dt, *J* = 11.7, 4.4 Hz, 1H), 2.08 (dd, *J* = 4.0, 1.7 Hz, 1H), 1.77 (dd, *J* = 14.0, 6.4 Hz, 2H), 1.66 – 1.60 (m, 2H), 1.53 – 1.48 (m, 2H), 1.43 (d, *J* = 6.7 Hz, 2H), 1.03 (t, *J* = 7.1 Hz, 3H). ^{13}C NMR (101 MHz, Acetone-d_6) δ 174.00, 158.50, 157.38, 157.24, 140.90, 137.51, 131.54, 130.62, 129.57, 129.11, 128.51, 124.40, 123.76, 115.64, 115.44, 114.55, 84.42, 82.70, 67.76, 61.33, 46.41, 33.27, 30.39, 28.92, 28.66, 25.59, 24.70, 14.05. HRMS (ESI) calcd for $C_{33}H_{37}NO_8S$ $[M + Na]^+$, 630.2132; found 630.2135.

*8-(4-(N-Ethyl-5,6-bis(4-hydroxyphenyl)-7-oxabicyclo[2.2.1]hept-5-ene-2-sulfonamido)phenoxy)octanoic acid (**17s**)*: Yellow solid, 70% yield, mp 104-106 °C. ^{1}H NMR (400 MHz, Acetone-d_6) δ 7.26 (dd, *J* = 12.0, 8.4 Hz, 2H), 7.24 – 7.18 (m, 4H), 6.85 (dd, *J* = 11.1, 8.8 Hz, 4H), 6.80 (d, *J* = 8.6 Hz, 2H), 5.48 (s, 1H), 5.33 (d, *J* = 3.9 Hz, 1H), 3.99 (t, *J* = 6.4 Hz, 2H), 3.78 (q, *J* = 7.0 Hz, 2H), 3.48 (dd, *J* = 8.3, 4.5 Hz, 1H), 2.31 (t, *J* = 7.4 Hz, 2H), 2.20 (dt, *J* = 11.7, 4.4 Hz, 1H), 2.10 – 2.06 (m, 1H), 1.81 – 1.74 (m, 2H), 1.65 – 1.59 (m, 2H), 1.50 (d, *J* = 7.0 Hz, 2H), 1.40 (d, *J* = 3.6 Hz, 4H), 1.03 (t, *J* = 7.0 Hz, 3H). ^{13}C NMR (101 MHz, Acetone-d_6) δ 174.11, 158.52, 157.29, 140.90, 137.50, 131.53, 130.62, 129.10, 128.51, 124.38, 115.68, 115.48, 114.56, 84.42, 82.70, 67.83, 61.35, 46.42, 33.35, 30.40, 28.88, 25.73, 24.72, 14.06. HRMS (ESI) calcd for $C_{34}H_{39}NO_8S$ $[M + Na]^+$, 644.2289; found 644.2287.

*11-(4-(N-Ethyl-5,6-bis(4-hydroxyphenyl)-7-oxabicyclo[2.2.1]hept-5-ene-2-sulfonamido)phenoxy)undecanoic acid (**17t**)*: Yellow solid, 72% yield, mp 92-94 °C. ^{1}H NMR (400 MHz, Acetone-d_6) δ 7.28 (dd, *J* = 21.5, 9.6 Hz, 2H), 7.25 – 7.18 (m, 4H), 6.91 – 6.82 (m, 4H), 6.80 (d, *J* = 8.5 Hz, 2H), 5.48 (s, 1H), 5.33 (d, *J* = 4.1 Hz, 1H), 3.98 (t, *J* = 6.4 Hz, 3H), 3.78 (dd, *J* = 13.9, 6.9 Hz, 2H), 3.48 (dd, *J* = 8.2, 4.4 Hz, 1H), 2.29 (t, *J* = 7.4 Hz, 2H), 2.24 – 2.17 (m, 1H), 2.07 (s, 1H), 1.80 – 1.74 (m, 2H), 1.63 – 1.57 (m, 2H), 1.48 (s, 2H), 1.34 (s, 10H), 1.03 (t, *J* = 7.1 Hz, 3H). ^{13}C NMR (101 MHz, Acetone-d_6) δ 173.99, 158.52, 157.28, 140.90, 137.52, 131.54, 130.61, 129.09, 128.51, 124.40, 123.76, 115.67, 115.47, 114.54, 84.42, 82.70, 67.85, 61.37, 46.41, 33.35, 30.40, 29.29, 29.09, 28.96, 25.87, 24.78, 14.05. HRMS (ESI) calcd for $C_{37}H_{45}NO_8S$ $[M + Na]^+$, 686.2758; found 686.2760.

4.3 Biological assays

4.3.1 Estrogen receptor binding affinity.

Relative binding affinities were determined by a competitive fluorometric binding assay. Briefly, 40 nM of a fluorescence tracer and 0.8 μM purified human ERα ligand binding domain (LBD) were diluted in 100 mM potassium phosphate buffer (pH 7.4) containing 100 μg/mL bovine gamma globulin (Sigma-Aldrich, MO). Incubations were performed for 2 h at room temperature (25 °C) in the dark. We then used a Cytation 3 microplate reader (BioTek) to measure fluorescence polarization values. The binding affinities are expressed as relative

binding affinity (RBA) values with the RBA of 17β-estradiol set to 100%. The values given are the average ± range of two independent determinations. K_i values were calculated according to the following equation: $Ki = (100/RBA) \times K_d$.

4.3.2 Cell culture and cell viability assay.

The MCF-7 human breast cancer cell line was obtained from ATCC. Cells were maintained in DMEM with 10% FBS. For all experiments, the cells were grown in 96-well microtiter plates (Nest Biotech Co., China) with the appropriate ligand in triplicate for 72 h. MTT colorimetric tests (Biosharp, China) were employed to determine cell viability per manufacturer's instructions. IC_{50} values were calculated according to the following equation using Origin 8 software: Y = 100% inhibition + (0% inhibition – 100% inhibition)/(1 + $10^{[(\log IC_{50}-X)\times Hillslope]}$), where Y = fluorescence value, X = $\log^{[inhibitor]}$.

4.3.3 Western blot analyses of ERα protein levels in MCF-7 cells.

Cells were incubated with DMSO or compound (10 μM) for 20 h. Whole protein was extracted and ERα protein levels were analyzed by Western blotting. Proteins from cell lysates were separated electrophoretically using 8% SDS-PAGE Gels. Gels were then electroblotted onto polyvinylidene fluoride (PVDF) membranes (Life Technologies). After blocking with 5% skimmed milk, the membranes were incubated with Rabbit anti-ERα antibody (1:1000, CST) and mouse Anti-β-actin antibody (1:10000, ABclonal Technology). Then, membranes were washed with 0.1% tween-20 in TBS and incubated with goat anti rabbit secondary antibody (Thermo). After washing with 0.1% tween-20 in TBS, they were tested by ECL. All the bands were quantitatively analyzed by Quantity One, and the vehicle was set as 100%.

4.4 Molecular modeling.

The crystal structure of ERα LBD (PDB 5kcc) was obtained from the PDB, and all water molecules were removed. We used AutoDock software (version 4.2) to dock compounds **17e**

into the three-dimensional structure of ERα LBD. The crystallographic coordinates of **17e** was created by Chemoffice. Preparations of all ligands and the protein were performed with AutoDockTools (ADT). A docking cube with edges of 66, 66, and 60 Å in the X, Y, and Z dimensions, respectively (a grid spacing of 0.375 Å). The search parameters were determined using the Genetic Algorithm and the output based on the Lamarckian genetic algorithm (LGA). The figures were prepared using MOE.

4.5 Pharmacokinetic study.

Sprague-Dawley rats were used for the pharmacokinetic study on compound **17e**. All procedures in animal studies were carried out in compliance with the Guide for the Care and Use Committee (Permit No: SCXK (Hu) 2018-0006). Compound **17e** was dissolved in Saline with 5% DMSO and 40% PEG400. After fasting overnight, the animals were administered a single dose of 3 mg/kg **17e** by *iv* and 10 mg/mL **17e** by *po*. After drug administration, blood samples were collected from the orbital sinus of the rat at various time points with each group. An aliquot of 50 μL plasma sample was protein precipitated with 250 μL MeOH in which contains 200 ng/mL IS. The mixture was vortexed for 2 min and centrifuged at 12000 rpm for 5 min. An aliquot of 5 μL supernatant was injected for LC-MS/MS analysis.

Appendix A. Supplementary data

Supplementary data related to this article can be found at https://doi.org/

Acknowledgements:

We are grateful to the NSFC (81773557 and 81573279), the Major Project of Technology Innovation Program of Hubei Province (2016ACA126, 2016ACA148, 2018ACA123), the NSFHP (2017CFA024), the Fundamental Research Funds for the Central Universities of China (2042017kf0288), and the Open Research Fund Program of the Hubei Province Engineering and Technology Research Center for Fluorinated Pharmaceuticals for supporting this research.

References

[1] J.A. Katzenellenbogen, C.G. Mayne, B.S. Katzenellenbogen, G.L. Greene, S. Chandarlapaty, Structural underpinnings of oestrogen receptor mutations in endocrine therapy resistance, Nat. Rev. Cancer 18 (2018) 377-388.

[2] K. Tryfonidis, D. Zardavas, B.S. Katzenellenbogen, M. Piccart, Endocrine treatment in breast cancer: Cure, resistance and beyond, Cancer Treat. Rev. 50 (2016) 68-81.

[3] W. Lv, J. Liu, T.C. Skaar, E. O'Neill, G. Yu, D.A. Flockhart, M. Cushman, Synthesis of Triphenylethylene Bisphenols as Aromatase Inhibitors That Also Modulate Estrogen Receptors, J. Med. Chem. 59 (2016) 157-170.

[4] D. Ghosh, J. Lo, D. Morton, D. Valette, J. Xi, J. Griswold, S. Hubbell, C. Egbuta, W. Jiang, J. An, H.M. Davies, Novel aromatase inhibitors by structure-guided design, J. Med. Chem. 55 (2012) 8464-8476.

[5] M.G. Ferlin, D. Carta, R. Bortolozzi, R. Ghodsi, A. Chimento, V. Pezzi, S. Moro, N. Hanke, R.W. Hartmann, G. Basso, G. Viola, Design, synthesis, and structure-activity relationships of azolylmethylpyrroloquinolines as nonsteroidal aromatase inhibitors, J. Med. Chem. 56 (2013) 7536-7551.

[6] G.G. Chen, Q. Zeng, G.M. Tse, Estrogen and its receptors in cancer, Med. Res. Rev. 28 (2008) 954-974.

[7] E.K. Shanle, W. Xu, Endocrine disrupting chemicals targeting estrogen receptor signaling: identification and mechanisms of action, Chem. Res. Toxicol. 24 (2011) 6-19.

[8] R. Singla, K. Prakash, K. Bihari Gupta, S. Upadhyay, M. Dhiman, V. Jaitak, Identification of novel indole based heterocycles as selective estrogen receptor modulator, Bioorg. Chem. 79 (2018) 72-88.

[9] J.N. Mills, A.C. Rutkovsky, A. Giordano, Mechanisms of resistance in estrogen receptor positive breast cancer: overcoming resistance to tamoxifen/aromatase inhibitors, Curr. Opin.Pharmacol. 41 (2018) 59-65.

[10] A. Nardone, C. De Angelis, M.V. Trivedi, C.K. Osborne, R. Schiff, The changing role of ER in endocrine resistance, Breast, 24 Suppl 2 (2015) S60-66.

[11] K. Merenbakh-Lamin, N. Ben-Baruch, A. Yeheskel, A. Dvir, L. Soussan-Gutman, R. Jeselsohn, R. Yelensky, M. Brown, V.A. Miller, D. Sarid, S. Rizel, B. Klein, T. Rubinek, I. Wolf, D538G mutation in estrogen receptor-alpha: A novel mechanism for acquired endocrine resistance in breast cancer, Cancer Res. 73 (2013) 6856-6864.

[12] A.C. Lai, C.M. Crews, Induced protein degradation: an emerging drug discovery paradigm, Nat. Rev. Drug Discov. 16 (2017) 101-114.

[13] G.M. Burslem, C.M. Crews, Small-Molecule Modulation of Protein Homeostasis, Chem. Rev. 117 (2017) 11269-11301.

[14] M.M. Boisen, C.L. Andersen, S. Sreekumar, A.M. Stern, S. Oesterreich, Treating gynecologic malignancies with selective estrogen receptor downregulators (SERDs): promise and challenges, Mol. Cell. Endocrinol. 418 (2015) 322-333.

[15] D.P. McDonnell, S.E. Wardell, J.D. Norris, Oral Selective Estrogen Receptor Downregulators (SERDs), a Breakthrough Endocrine Therapy for Breast Cancer, J. Med. Chem. 58 (2015) 4883-4887.

[16] L. Wang, V.S. Guillen, N. Sharma, K. Flessa, J. Min, K.E. Carlson, W. Toy, S. Braqi, B.S. Katzenellenbogen, J.A. Katzenellenbogen, S. Chandarlapaty, A. Sharma, New Class of Selective Estrogen Receptor Degraders (SERDs): Expanding the Toolbox of PROTAC Degrons, ACS Med. Chem. Lett. 9 (2018) 803-808.

[17] G.S. Tria, T. Abrams, J. Baird, H.E. Burks, B. Firestone, L.A. Gaither, L.G. Hamann, G. He, C.A. Kirby, S. Kim, F. Lombardo, K.J. Macchi, D.P. McDonnell, Y. Mishina, J.D. Norris, J. Nunez, C. Springer, Y. Sun, N.M. Thomsen, C. Wang, J. Wang, B. Yu, C.L. Tiong-Yip, S. Peukert, Discovery of LSZ102, a Potent, Orally Bioavailable Selective Estrogen Receptor Degrader (SERD) for the Treatment of Estrogen Receptor Positive Breast Cancer, J. Med. Chem. 61 (2018) 2837-2864.

[18] J. Nagasawa, S. Govek, M. Kahraman, A. Lai, C. Bonnefous, K. Douglas, J. Sensintaffar, N. Lu, K. Lee, A. Aparicio, J. Kaufman, J. Qian, G. Shao, R. Prudente, J.D. Joseph, B. Darimont, D. Brigham, K. Maheu, R. Heyman, P.J. Rix, J.H. Hager, N.D. Smith, Identification of an Orally Bioavailable Chromene-Based Selective Estrogen Receptor Degrader (SERD) That Demonstrates Robust Activity in a Model of Tamoxifen-Resistant Breast Cancer, J. Med. Chem. 61 (2018) 7917-7928.

[19] A. Di Leo, G. Jerusalem, L. Petruzelka, R. Torres, I.N. Bondarenko, R. Khasanov, D. Verhoeven, J.L. Pedrini, I. Smirnova, M.R. Lichinitser, K. Pendergrass, S. Garnett, J.P. Lindemann, F. Sapunar, M. Martin, Results of the CONFIRM phase III trial comparing fulvestrant 250 mg with fulvestrant 500 mg in postmenopausal women with estrogen receptor-positive advanced breast cancer, J. Clin. Oncol. 28 (2010) 4594-4600.

[20] M. van Kruchten, E.G. de Vries, A.W. Glaudemans, M.C. van Lanschot, M. van Faassen, I.P. Kema, M. Brown, C.P. Schroder, E.F. de Vries, G.A. Hospers, Measuring residual estrogen receptor availability during fulvestrant therapy in patients with metastatic breast cancer, Cancer Discov. 5 (2015) 72-81.

[21] R. Xiong, J. Zhao, L.M. Gutgesell, Y. Wang, S. Lee, B. Karumudi, H. Zhao, Y. Lu, D.A. Tonetti, G.R. Thatcher, Novel Selective Estrogen Receptor Downregulators (SERDs) Developed against Treatment-Resistant Breast Cancer, J. Med. Chem. 60 (2017) 1325-1342.

[22] N.M. O'Boyle, I. Barrett, L.M. Greene, M. Carr, D. Fayne, B. Twamley, A.J.S. Knox, N.O. Keely, D.M. Zisterer, M.J. Meegan, Lead Optimization of Benzoxepin-Type Selective Estrogen Receptor (ER) Modulators and Downregulators with Subtype-Specific ERalpha and ERbeta Activity, J. Med. Chem. 61 (2018) 514-534.

[23] J. Liu, S. Zheng, S. Guo, C. Zhang, Q. Zhong, Q. Zhang, P. Ma, E.V. Skripnikova, M.R. Bratton, T.E. Wiese, G. Wang, Rational Design of a Boron-Modified Triphenylethylene (GLL398) as an Oral Selective

Estrogen Receptor Downregulator, ACS Med. Chem. Lett. 8 (2017) 102-106.

[24] H.E. Burks, T. Abrams, C.A. Kirby, J. Baird, A. Fekete, L.G. Hamann, S. Kim, F. Lombardo, A. Loo, D. Lubicka, K. Macchi, D.P. McDonnell, Y. Mishina, J.D. Norris, J. Nunez, C. Saran, Y. Sun, N.M. Thomsen, C. Wang, J. Wang, S. Peukert, Discovery of an Acrylic Acid Based Tetrahydroisoquinoline as an Orally Bioavailable Selective Estrogen Receptor Degrader for ERalpha+ Breast Cancer, J. Med. Chem. 60 (2017) 2790-2818.

[25] T. Shoda, M. Kato, T. Fujisato, T. Misawa, Y. Demizu, H. Inoue, M. Naito, M. Kurihara, Synthesis and evaluation of raloxifene derivatives as a selective estrogen receptor down-regulator, Bioorg. Med. Chem. 24 (2016) 2914-2919.

[26] T. Shoda, K. Okuhira, M. Kato, Y. Demizu, H. Inoue, M. Naito, M. Kurihara, Design and synthesis of tamoxifen derivatives as a selective estrogen receptor down-regulator, Bioorg. Med. Chem. Lett. 24 (2014) 87-89.

[27] A. Lai, M. Kahraman, S. Govek, J. Nagasawa, C. Bonnefous, J. Julien, K. Douglas, J. Sensintaffar, N. Lu, K.J. Lee, A. Aparicio, J. Kaufman, J. Qian, G. Shao, R. Prudente, M.J. Moon, J.D. Joseph, B. Darimont, D. Brigham, K. Grillot, R. Heyman, P.J. Rix, J.H. Hager, N.D. Smith, Identification of GDC-0810 (ARN-810), an Orally Bioavailable Selective Estrogen Receptor Degrader (SERD) that Demonstrates Robust Activity in Tamoxifen-Resistant Breast Cancer Xenografts, J. Med. Chem. 58 (2015) 4888-4904.

[28] Y.L. Wu, X. Yang, Z. Ren, D.P. McDonnell, J.D. Norris, T.M. Willson, G.L. Greene, Structural basis for an unexpected mode of SERM-mediated ER antagonism, Mol. Cell. 18 (2005) 413-424.

[29] K. Cyrus, M. Wehenkel, E.Y. Choi, H. Lee, H. Swanson, K.B. Kim, Jostling for position: optimizing linker location in the design of estrogen receptor-targeting PROTACs, Chem.Med. Chem. 5 (2010) 979-985.

[30] Y. Demizu, K. Okuhira, H. Motoi, A. Ohno, T. Shoda, K. Fukuhara, H. Okuda, M. Naito, M. Kurihara, Design and synthesis of estrogen receptor degradation inducer based on a protein knockdown strategy, Bioorg. Med. Chem. Lett. 22 (2012) 1793-1796.

[31] Y. Jiang, Q. Deng, H. Zhao, M. Xie, L. Chen, F. Yin, X. Qin, W. Zheng, Y. Zhao, Z. Li, Development of Stabilized Peptide-Based PROTACs against Estrogen Receptor alpha, ACS Chem. Biol. 13 (2018) 628-635.

[32] R.P. Wurz, K. Dellamaggiore, H. Dou, N. Javier, M.C. Lo, J.D. McCarter, D. Mohl, C. Sastri, J.R. Lipford, V.J. Cee, A "Click Chemistry Platform" for the Rapid Synthesis of Bispecific Molecules for Inducing Protein Degradation, J. Med. Chem. 61 (2018) 453-461.

[33] N. Shibata, K. Nagai, Y. Morita, O. Ujikawa, N. Ohoka, T. Hattori, R. Koyama, O. Sano, Y. Imaeda, H. Nara, N. Cho, M. Naito, Development of Protein Degradation Inducers of Androgen Receptor by Conjugation of Androgen Receptor Ligands and Inhibitor of Apoptosis Protein Ligands, J. Med. Chem. 61 (2018) 543-575.

[34] M. Schiedel, D. Herp, S. Hammelmann, S. Swyter, A. Lehotzky, D. Robaa, J. Olah, J. Ovadi, W. Sippl, M.

Jung, Chemically Induced Degradation of Sirtuin 2 (Sirt2) by a Proteolysis Targeting Chimera (PROTAC) Based on Sirtuin Rearranging Ligands (SirReals), J. Med. Chem. 61 (2018) 482-491.

[35] K.A. Dreher, J. Brown, R.E. Saw, J. Callis, The Arabidopsis Aux/IAA protein family has diversified in degradation and auxin responsiveness, Plant cell 18 (2006) 699-714.

[36] K.M. Bonger, L.C. Chen, C.W. Liu, T.J. Wandless, Small-molecule displacement of a cryptic degron causes conditional protein degradation, Nat. Chem. Biol. 7 (2011) 531-537.

[37] M. Zhu, C. Zhang, J.C. Nwachukwu, S. Srinivasan, V. Cavett, Y. Zheng, K.E. Carlson, C. Dong, J.A. Katzenellenbogen, K.W. Nettles, H.B. Zhou, Bicyclic core estrogens as full antagonists: synthesis, biological evaluation and structure-activity relationships of estrogen receptor ligands based on bridged oxabicyclic core arylsulfonamides, Org. Biomol. Chem. 10 (2012) 8692-8700.

[38] S. Srinivasan, J.C. Nwachukwu, N.E. Bruno, V. Dharmarajan, D. Goswami, I. Kastrati, S. Novick, J. Nowak, V. Cavett, H.B. Zhou, N. Boonmuen, Y. Zhao, J. Min, J. Frasor, B.S. Katzenellenbogen, P.R. Griffin, J.A. Katzenellenbogen, K.W. Nettles, Full antagonism of the estrogen receptor without a prototypical ligand side chain, Nat. Chem. Biol. 13 (2017) 111-118.

[39] Z. Hu, L. Yang, W. Ning, C. Tang, Q. Meng, J. Zheng, C. Dong, H.B. Zhou, A high-affinity subtype-selective fluorescent probe for estrogen receptor beta imaging in living cells, Chem. Commun. 54 (2018) 3887-3890.

[40] L. Yang, Q.Y. Meng, Z.Y. Hu, W.T. Ning, J. Zheng, C.E. Dong, H.B. Zhou, Estrogen receptor sensing in living cells by a high affinity turn-on fluorescent probe, Sensor Actuat B-Chem. 272 (2018) 589-597.

[41] W. Ning, Z. Hu, C. Tang, L. Yang, S. Zhang, C. Dong, J. Huang, H.B. Zhou, Novel Hybrid Conjugates with Dual Suppression of Estrogenic and Inflammatory Activities Display Significantly Improved Potency against Breast Cancer, J. Med. Chem. 61 (2018) 8155-8173.

[42] C. Tang, C. Li, S. Zhang, Z. Hu, J. Wu, C. Dong, J. Huang, H.B. Zhou, Novel Bioactive Hybrid Compound Dual Targeting Estrogen Receptor and Histone Deacetylase for the Treatment of Breast Cancer, J. Med. Chem. 58 (2015) 4550-4572.

[43] H.B. Zhou, J.S. Comninos, F. Stossi, B.S. Katzenellenbogen, J.A. Katzenellenbogen, Synthesis and evaluation of estrogen receptor ligands with bridged oxabicyclic cores containing a diarylethylene motif: estrogen antagonists of unusual structure, J. Med. Chem. 48 (2005) 7261-7274.

[44] Y. Zheng, C. Wang, C. Li, J. Qiao, F. Zhang, M. Huang, W. Ren, C. Dong, J. Huang, H.B. Zhou, Discovery of novel SERMs with a ferrocenyl entity based on the oxabicyclo[2.2.1]heptene scaffold and evaluation of their antiproliferative effects in breast cancer cells, Org. Biomol. Chem. 10 (2012) 9689-9699.

[45] N. Sharma, K.E. Carlson, J.C. Nwachukwu, S. Srinivasan, A. Sharma, K.W. Nettles, J.A. Katzenellenbogen, Exploring the Structural Compliancy versus Specificity of the Estrogen Receptor Using Isomeric

Three-Dimensional Ligands, ACS Chem. Biol. 12 (2017) 494-503.

Highlights

- A series of novel SERDs with excellent ER degradation efficacy have been discovered.
- These findings simplified the structure of currently available degrons and provide new possibility for discovering novel PROTACs.
- Molecular docking analysis illustrates the interaction of basic side chain of these compounds with ERα, which may implicate a new mechanism of action for this type of SERDs.